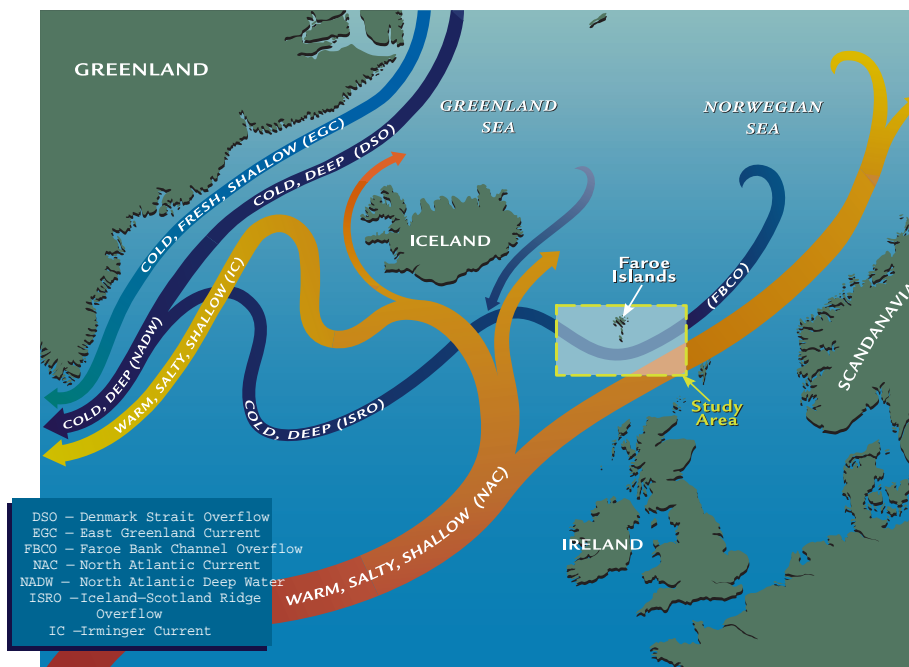


A Report of  
XCP and CTD data taken during  
June, 2001, RRS Discovery cruise 247B  
A Process Study of the Faroe Bank Channel Overflow

April 30, 2001



CoPIs: James F. Price, Woods Hole Oceanographic Institution  
Thomas B. Sanford, Applied Physics Laboratory, Univ. of Washington  
Cecilie Mauritzen, Woods Hole Oceanographic Institution  
Mark Prater, Graduate School of Oceanography, Univ. of Rhode Island

# 1 Overview of the Field Program

Faroe Bank Channel (FBC) is the deepest passage between the Norwegian-Greenland Sea and the North Atlantic Ocean (Figure 1). There is observed to be a quasi-steady overflow of dense water through FBC from the Norwegian-Greenland Sea into the abyssal North Atlantic at the rate of about 2 Sv. This dense overflow contributes significantly to the North East Atlantic Deep Water, which in turn is a major component of North Atlantic Deep Water. The FBC and its overflow have thus been of great interest to physical oceanography since its prominent role in deep water formation was appreciated in the 1950s.

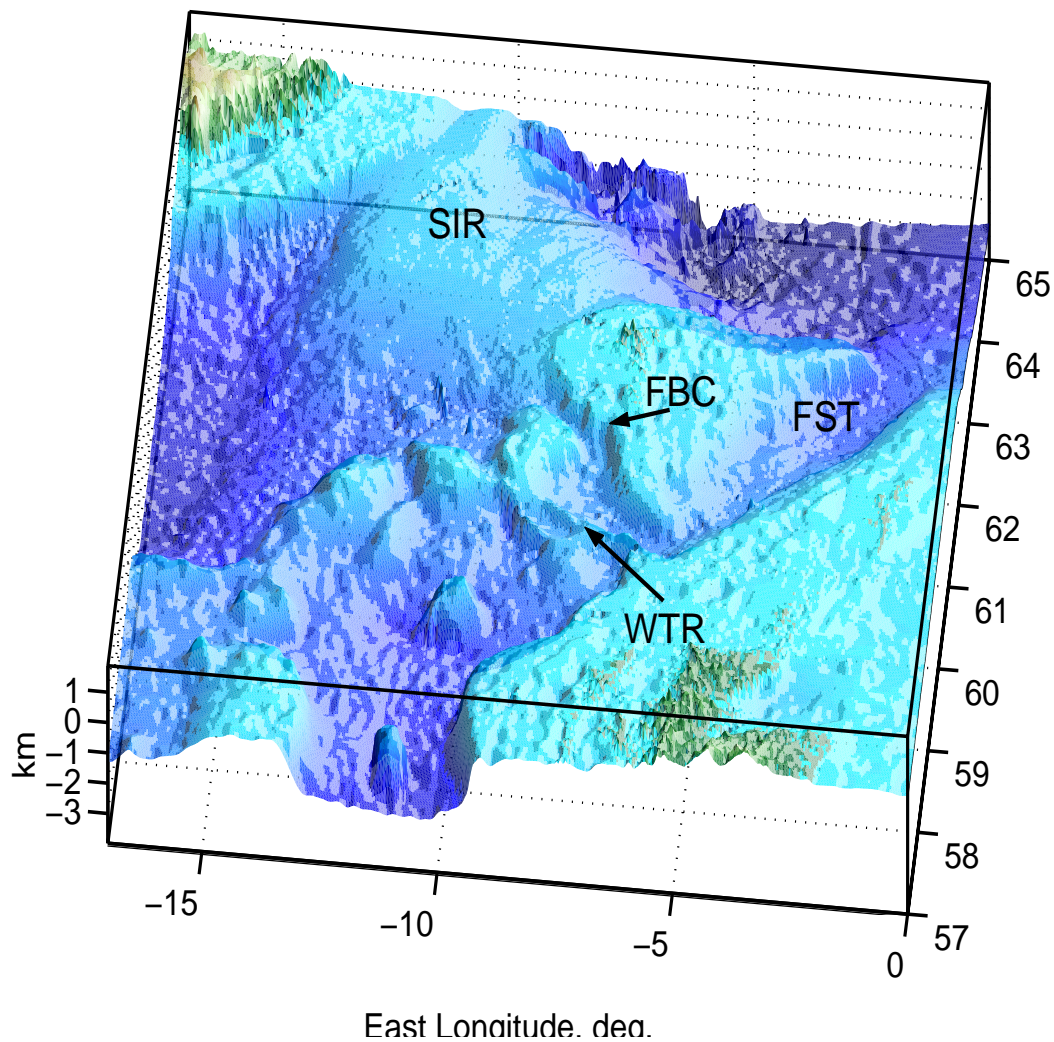


Figure 1: A 3-D view of the ocean sea floor in the Faroe Bank Channel region. SIR is the Scotland-Iceland Ridge, FBC is the Faroe Bank Channel, WTR is the Wyville-Thomson Ridge and FST is the Faroe Shetland Trough.

The goal of our field program was to acquire finely sampled measurements of currents and hydrography in the region several hundred kilometers up and downstream of the sill in FBC sufficient to address three specific questions: 1) What is the transport and momentum balance of the overflow? 2) How does the overflow water approach the sill southwest of the Faroe Islands, and is the overflow hydraulically controlled? 3) Where and how does mixing occur in the descending overflow?

Our starting point for addressing these questions was to acquire a data set sufficient to allow estimation of the volume, momentum, energy and vorticity budgets along the path of the overflow. Bottom stress and vertical mixing with overlying North Atlantic water were expected to be of significant importance for these budgets. The strategy of our field program was to make measurements along a number of transverse sections that spanned the overflow from the Faroe-Shetland Trough (the approach) to the southern flank of the Faroe-Iceland Ridge (the descending overflow). Currents were measured by expendable current profilers (XCP), ship-mounted acoustic Doppler current profiler (ADCP) and lowered acoustic Doppler current profiler (LADCP). Hydrographic properties were measured by CTD, and by acquiring discrete water samples (oxygen and nutrients).

The instruments performed as expected, and there was only a very small data loss due to mechanical failure or operator error. In total, we made 217 CTD/LADCP profiles, and 114 XCP profiles. Underway measurements were made by ADCP, and by a variety of navigation sensors (most importantly, differential GPS (DGPS)) and meteorological sensors. Bottom-following drifters were also deployed.

## 2 A Brief Chronology of the Cruise and the Sampling

Discovery departed Southampton on 5 June and steamed northward for the FBC region. The first task was to deploy a sound source at approx. 62N, 11W. Once this was accomplished, Discovery proceeded to the sill region of the FBC southwest of the Faroe Islands and began to sample along transverse sections labeled A, B, C, etc., in the order they were taken (Figure 2). These sections were made up of closely spaced CTD/XCP stations. The usual course of events was that an XCP was taken upon arrival at a CTD station. However, when we were at the end of a section and no longer within the dense overflow, we sometimes chose to withhold the XCP.

Sampling proceeded as planned until near the end of section D when a major low pressure weather system began to deepen and approach our area. Gale force winds caused the cessation of our work for a period of about 36 hrs (details of this are in the Ship's Operations Log). Once the winds abated, we resumed sampling to finish section D and then occupied section E. We judged that most of the mixing that was expected in the overflow had occurred by section E, and we never proceeded westward of about 10 40W.

Upon completion of E we returned to the sill section A, with the intent of continuing eastward to survey the approach of the overflow in the Faroe-Shetland Trough. We first reoccupied section A, calling the new section Ar, and discovered that a noticeable change - a considerably

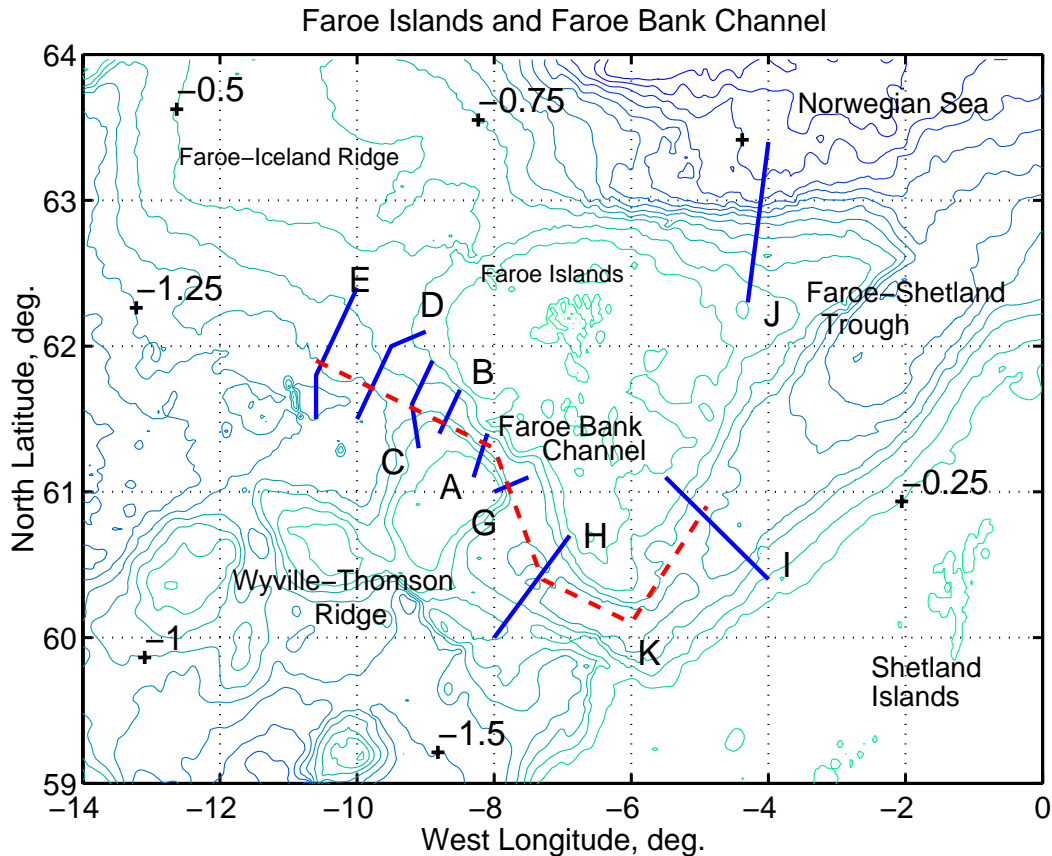


Figure 2: The approximate location of the CTD sections. There were about 30 CTD stations made as part of a time series or to close off the northern or southern end of sections that are not indicated here. The red dashed line labelled 'K' is a synthetic longitudinal section made up from stations selected from the transverse sections (the solid blue lines) and is intended to show the core of the overflow.

thicker and slightly colder overflow layer than at the time of A. We then sampled section G, and for the first time noticed what appeared to be high frequency (tidal or inertial period) fluctuation of the currents and hydrographic fields. This impression of variability was confirmed at section H, where we found quite large tidal or inertial variability that required repeated sampling. In all, we spent three days sampling on section H, or about two days more than anticipated. As part of section H we went to the Wyville-Thomson Ridge and observed a small and evidently fluctuating overflow (southward) across the ridge. We then sampled the approach along section I, where there was much less tidal/inertial variability, and proceeded to section J, completing the approach survey.

Given the significant change in the overflow from A to Ar we decided to occupy section A two more times, and then repeated sections C, D and E (C for the third time). On this second occupation of the descending overflow sections we found a somewhat larger volume of colder overflow water, indicating that the overflow had a greater transport during the second half the field program.

Compared to our original plan, we completed a slightly greater number of stations than anticipated. Also compared to the original plan, we used a greater fraction of these stations in a repeat sampling mode (e.g., we occupied section A four times vs. twice planned) on account of the evidence of temporal variability noted above. Similarly, we made seven sections on the approach; G twice, H three times, and I twice. Given the conditions we found, this repeat sampling seemed essential, though it was necessarily done at the expense of more extensive spatial coverage.

Sec A, 10 June  
Sec B, 10 June  
Sec C, 11 June  
Sec D first half, 12 June  
Storm delay, 13 June  
Sec D, resume, 14 June  
Sec E, 15 June  
Sec Ar, 16 June  
Sec Cr, 17 June  
Sec G, 18 June  
Sec Arr, 18 June  
Sec H, 20 June  
Sec Hr, 21 June  
Sec I, 22 June  
Sec J, 23 June  
Sec Arrr, 25 June  
Sec Crr, 27 June  
Sec Drr, 28 June  
Sec Er, 29 June  
Sec Gr, 29 June  
Sec Ir 30 June

The analysis of this data set will require many months of concerted effort, and we will not attempt here to forecast scientific conclusions. We are confident, however, that the horizontal resolution along sections is generally sufficient to resolve the mesoscale, transverse structure of the overflow, including the relative vorticity (an exception to this may be section H, where tidal/inertial variability was very large, though repeatedly sampled). As well, the changes observed from one section to the next appear 'coherent' (mapable) and hence we believe that the goal of estimating mixing-induced changes along the path of the descending overflow will also be achievable.

### 3 About This Report

This report is a working draft. It's main purpose is to disseminate results as quickly as possible to those involved in the project. This report is also available on an anonymous ftp site and so in that regard it is also in the public domain. However, we request that anyone wanting to use the report for anything other than their own information should contact one of the PIs for permission. The results shown here are fresh and untested; they may be significantly incomplete (the sampling of transport on section E, for example), and may even contain outright errors.

This report shows something less than half of the total data set. The full set of figures for all of the sections may be found on a web site, <http://www.whoi.edu/science/PO/people/jprice/> under a section entitled overflow models etc.; go directly to the ftp site. The graphics files are in eps format, and their content is coded into the file name as follows: the ctd section data are in five figures, say for section Ar - ctdAr1.eps is the potential temperature, ctdAr2.eps is salinity, 3 is the oxygen, 4 is the density, 5 is the T/S diagram and ctdmapAr.eps is the map of station locations. XCP data are in a similar form: xcpArr1.eps is the contour of velocity, xcpAr2.eps is the histogram of property transport and mapxcpAr.eps is the map of station locations (very similar to the CTD maps shown here).

### 4 Acknowledgements

This field project was made possible by the efforts of many skilled and dedicated people. XCP operations were set up by John Dunlap and James Girton, and assisted ably by Dicky Allison. The shipboard technical staff led by Jeff Benson was responsible for a flawless CTD and ADCP operation. The CTD data was logged by Deborah West-Mack assisted by the CTD watchstanders, Liz Hawker, Laura Cornick, Heather Deese, Avon Russell, Patricia Kassis and Peter Huybers. George Tupper managed much of the pre- and post-cruise logistical effort, and while at sea analyzed the salinity and oxygen samples. Dan Torres set up and supervised the LADCP operation. We are most grateful to Capt. Robin Plumley and the officers and crew of RRS Discovery for their steadfast support of all aspects of the project. Pre-cruise support provided by the Research Vessel Services staff, Edward Cooper, Andy Louch and Conor Mowlitz, is also greatly appreciated. Penny Foster organized travel and other pre-cruise administrative matters with efficiency and good humor. This project was funded by the U. S. National Science Foundation through grants OCE 99-06736 (to J. F. Price and C. Mauritzen) and OCE 99-11492 (to M. Prater).

### List of Figures

1	A 3-d perspective on the Faroe Bank Channel. . . . .	2
2	The approximate location of the CTD sections. . . . .	4

3	XCP profile from section Arr, in the narrow portion of Faroe Bank Channel.	10
4	XCP profile from section Cr. . . . .	11
5	XCP profile from section G, at the entrance to Faroe Bank Channel. . . . .	12
6	Station map of CTD section A. . . . .	13
7	CTD section A, T and S. . . . .	14
8	CTD section A, O and $\rho$ . . . . .	14
9	CTD section Ar, T and S. . . . .	15
10	CTD section Ar, O and $\rho$ . . . . .	15
11	CTD section Arr, T and S. . . . .	16
12	CTD section Arr, O and $\rho$ . . . . .	16
13	CTD section Arrr, T and S. . . . .	17
14	CTD section Arrr, O and $\rho$ . . . . .	17
15	T/S diagram from section A. . . . .	18
16	T/S diagram from section Ar. . . . .	19
17	T/S diagram from section Arr. . . . .	20
18	T/S diagram from section Arrr. . . . .	21
19	XCP section A. . . . .	22
20	XCP section Ar. . . . .	23
21	XCP section Arr. . . . .	24
22	XCP section Arrr. . . . .	25
23	3d view of XCP-measured currents from section Arr. . . . .	26
24	Transport by parameter class, section A. . . . .	27
25	Transport by parameter class, section Ar. . . . .	28
26	Transport by parameter class, section Arr. . . . .	29
27	Transport by parameter class, section Arrr. . . . .	30
28	Station map of CTD section Cr. . . . .	31
29	CTD section Cr, T and S. . . . .	32
30	CTD section Cr, O and $\rho$ . . . . .	32
31	T/S diagram from section Cr. . . . .	33

32	XCP section Cr. . . . .	34
33	Transport by parameter class, section Cr. . . . .	35
34	Station map of CTD section G. . . . .	36
35	CTD section Cr, T and S. . . . .	37
36	CTD section Cr, O and $\rho$ . . . . .	37
37	T/S diagram from section G. . . . .	38
38	XCP section G. . . . .	39
39	Transport by parameter class, section G. . . . .	40
40	CTD station map for section Er. . . . .	41
41	Potential temperature from section Er. . . . .	42
42	Salinity from section Er. . . . .	43
43	Oxygen from section Er. . . . .	44
44	Potential density from section Er. . . . .	45
45	T-S diagram from section Er. . . . .	46
46	XCP section Er. . . . .	47
47	Transport by parameter class, section Er. . . . .	48
48	CTD station map for section K, along the path of the Faroe Bank Channel overflow. . . . .	49
49	Potential temperature made up from CTD stations taken along the path of the Faroe Bank Channel overflow. . . . .	50
50	Salinity made up from CTD stations taken along the path of the Faroe Bank Channel overflow. . . . .	51
51	Dissolved oxygen made up from CTD stations taken along the path of the Faroe Bank Channel overflow. . . . .	52
52	Potential density made up from CTD stations taken along the path of the Faroe Bank Channel overflow. . . . .	53
53	T-S diagram from section K. . . . .	54
54	3d view of XCP currents. . . . .	55
55	Velocity-weighted transport of temperature, salinity and oxygen. . . . .	56
56	Transport and velocity-weighted density transport. . . . .	57
57	Bottom stress estimates. . . . .	58

58	The ensemble average of the near-bottom current. . . . .	59
59	The ensemble average rms of the deviation of the current from a log fit to each profile. . . . .	60

## 5 Selected XCP and CTD Profiles from the Faroe Bank Channel.

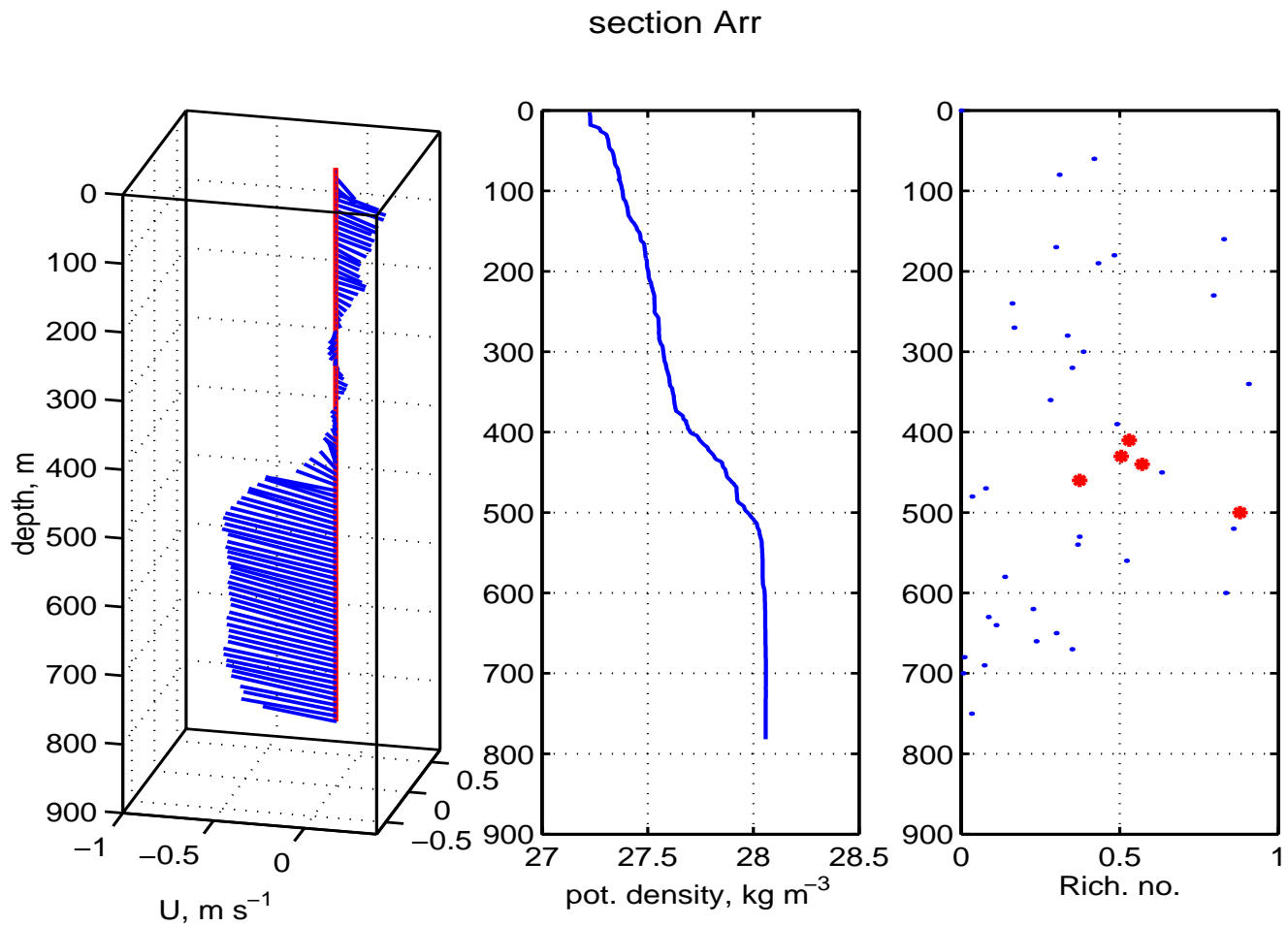


Figure 3: XCP and CTD profile data taken near the center of section Arr. (right most panel) Richardson number computed by vertical differencing over an interval of 10 m. The red dots on the Ri diagram indicate that the estimated density gradient exceeded  $0.001 \text{ kg m}^{-1}$ .

## section Cr

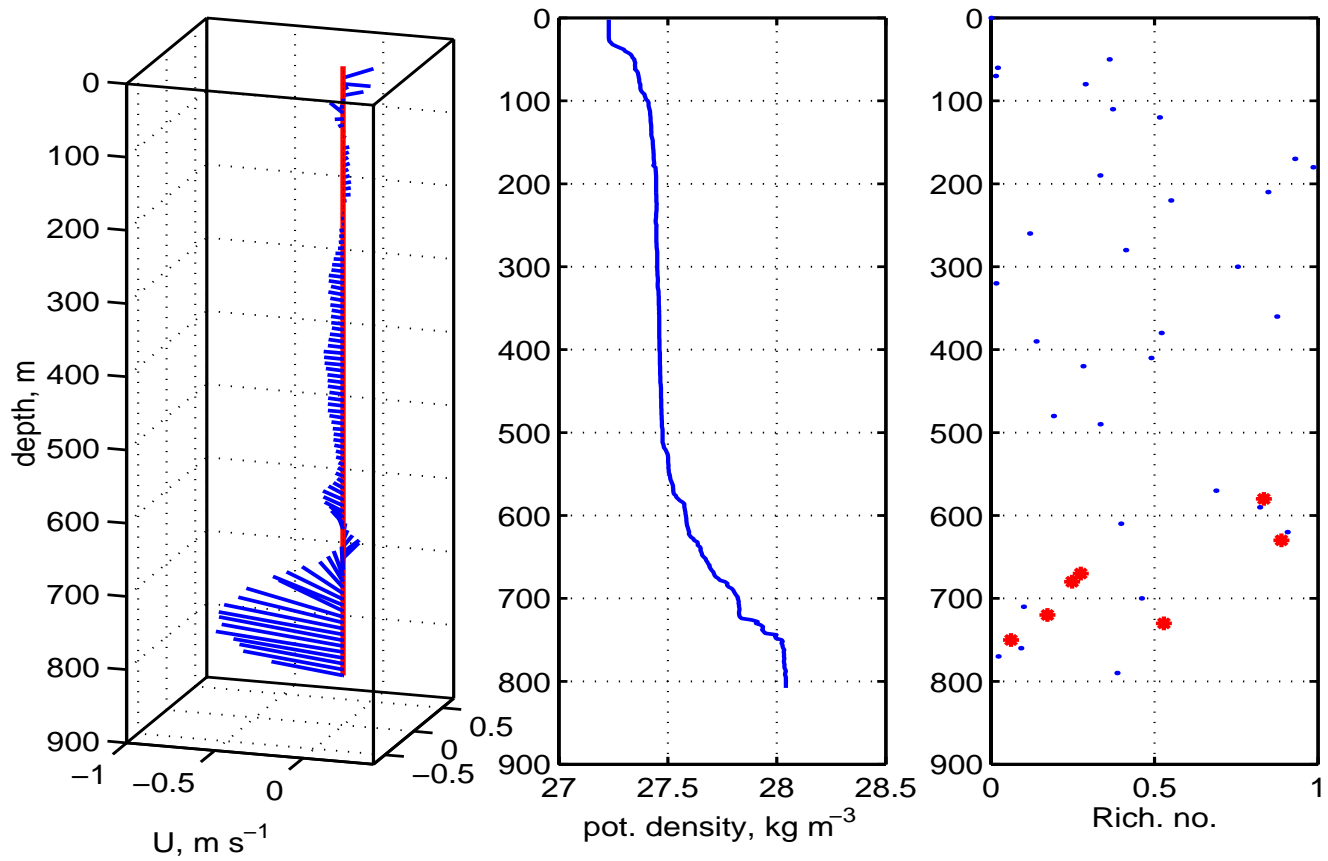


Figure 4: XCP and CTD profile data taken near the center of section Cr. (right most panel) Richardson number computed by vertical differencing over an interval of 10 m. The red dots on the Ri diagram indicate that the estimated density gradient exceeded  $0.001 \text{ kg m}^{-1}$ .

## section G

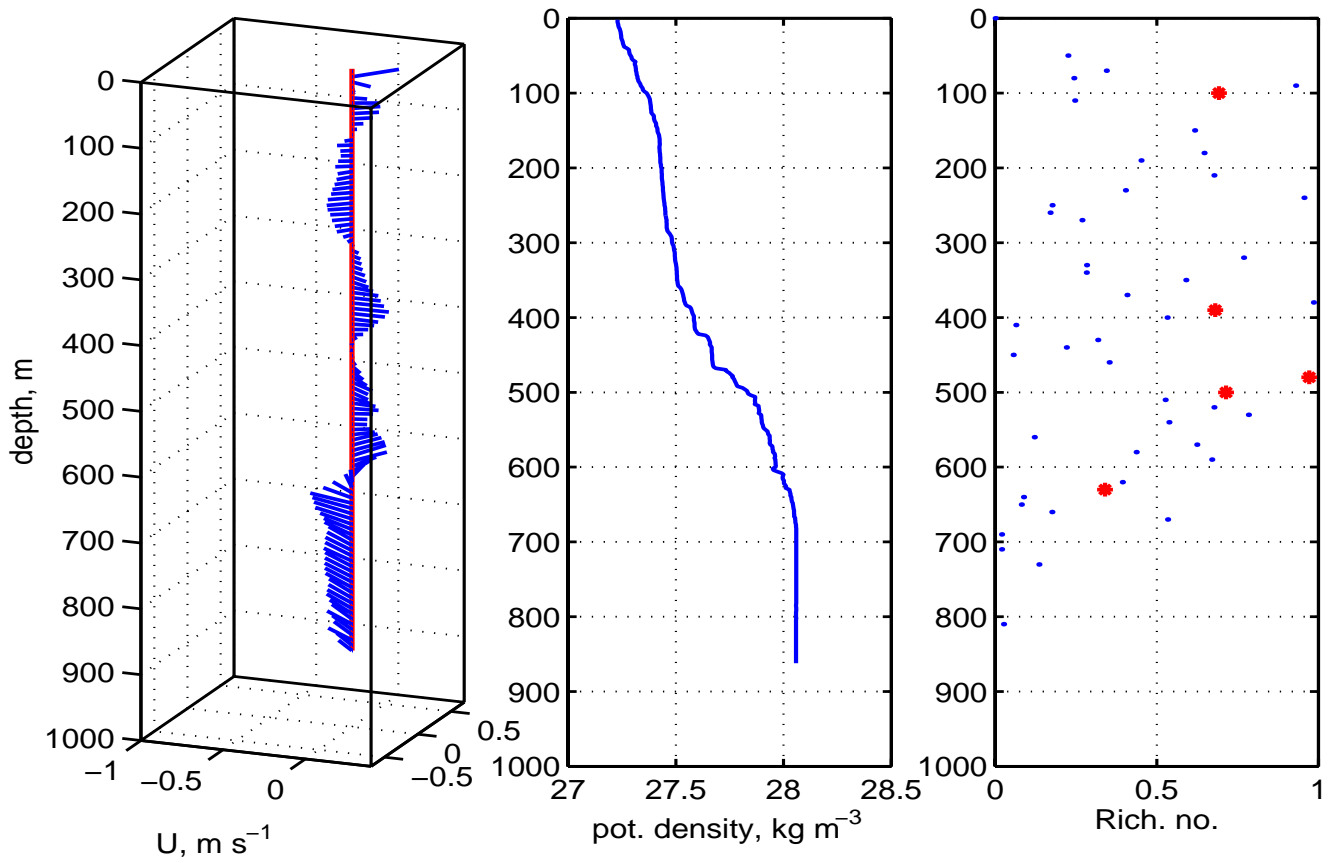


Figure 5: XCP and CTD profile data taken near the center of section G. (right most panel) Richardson number computed by vertical differencing over an interval of 10 m. The red dots on the Ri diagram indicate that the estimated density gradient exceeded  $0.001 \text{ kg m}^{-1}$ .

## 6 Section A Repeat Sampling.

Section A, located near the center of the Faroe Bank Channel (see figure 6) was occupied four times during the cruise. These repeated sections are shown together in a common format so that temporal variability may be assessed.

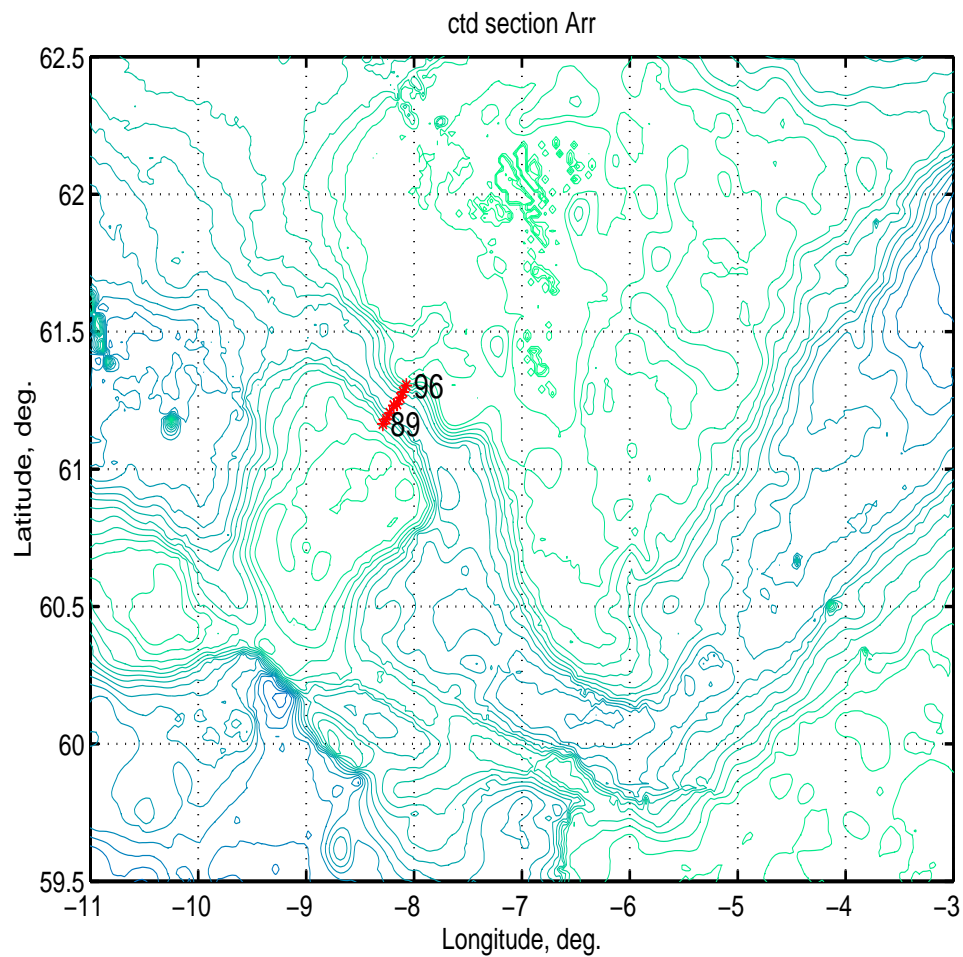


Figure 6: Station locations for section Arr; the other occupations of this section, A, Ar and Arr, were along the same line.

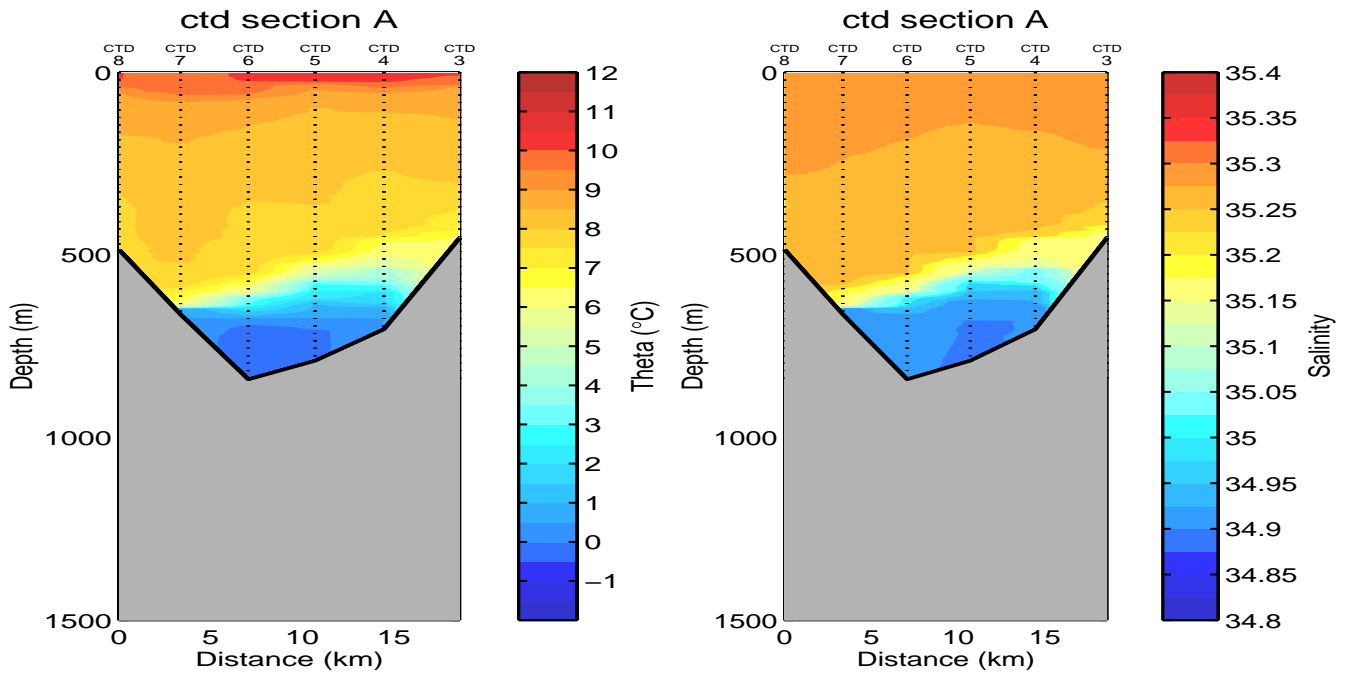


Figure 7: A section of potential temperature (left) and salinity (right) made up from CTD stations taken across the narrow part of the Faroe Bank Channel overflow (see Figure 6 for details of station locations). This view is to the west and in the direction of the overflow current.

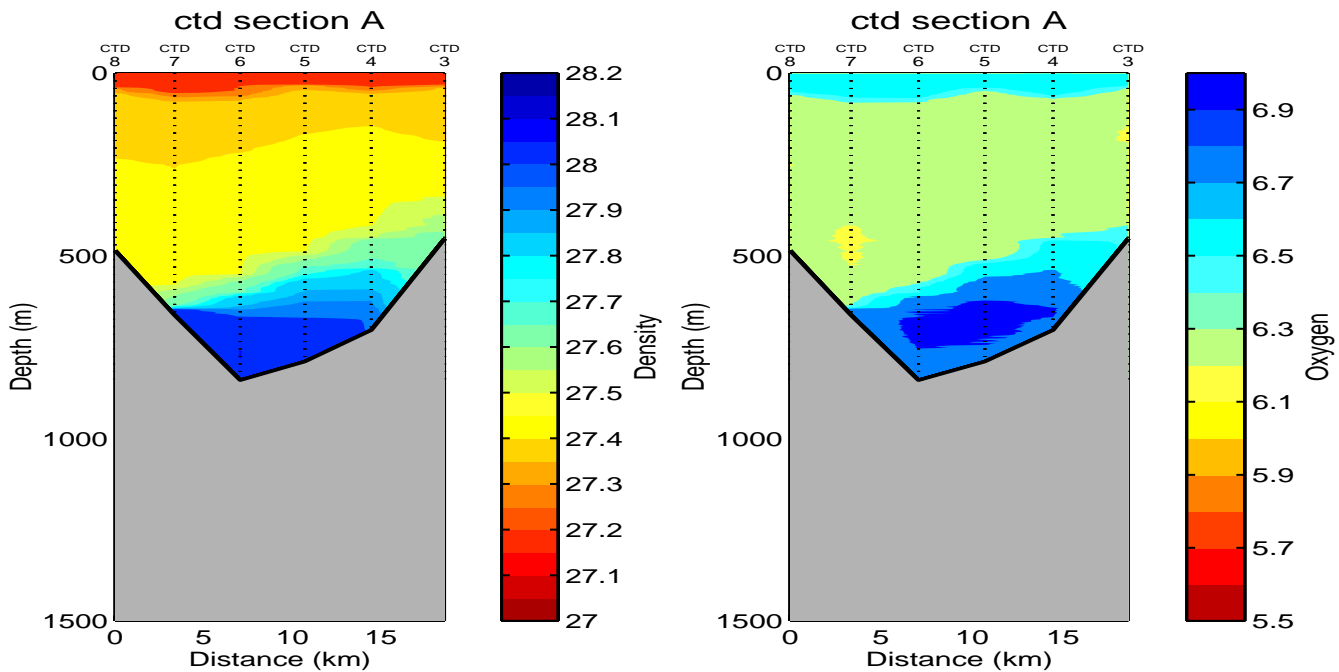


Figure 8: A section of potential density (left) and oxygen concentration (right) made up from CTD stations taken across the narrow part of the Faroe Bank Channel overflow (see Figure 6 for the station locations for this section A). This view is to the west, or in the direction of the overflow current.

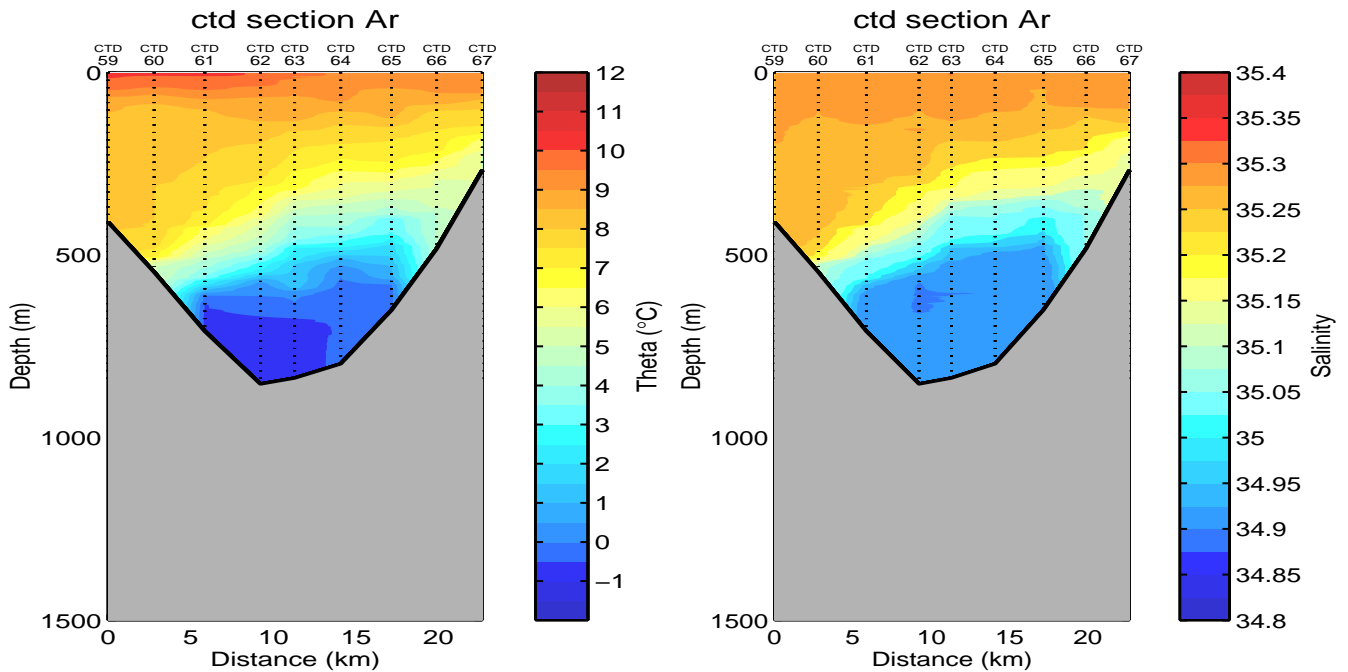


Figure 9: A section of potential temperature (left) and salinity (right) made up from CTD stations taken across the narrow part of the Faroe Bank Channel overflow (see Figure 6 for details of station locations). This view is to the west and in the direction of the overflow current.

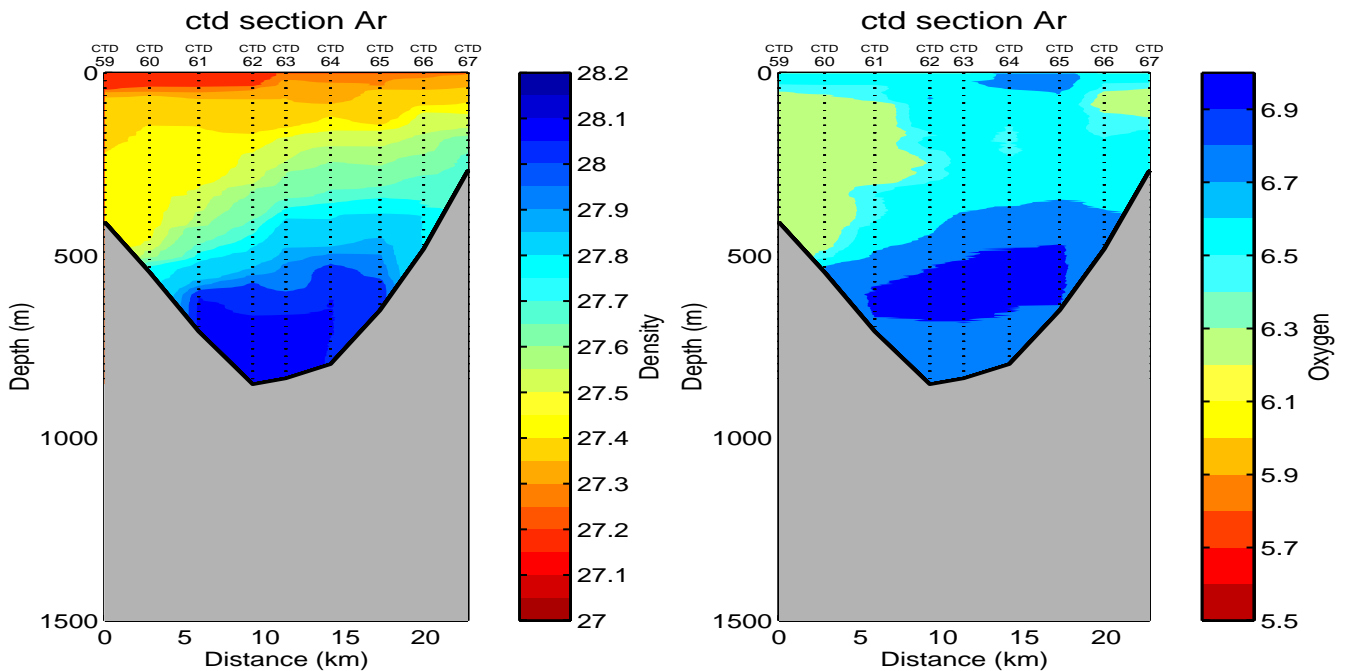


Figure 10: A section of potential density (left) and oxygen concentration (right) made up from CTD stations taken across the narrow part of the Faroe Bank Channel overflow (see Figure 6 for details of station locations). This view is to the west, or in the direction of the overflow current.

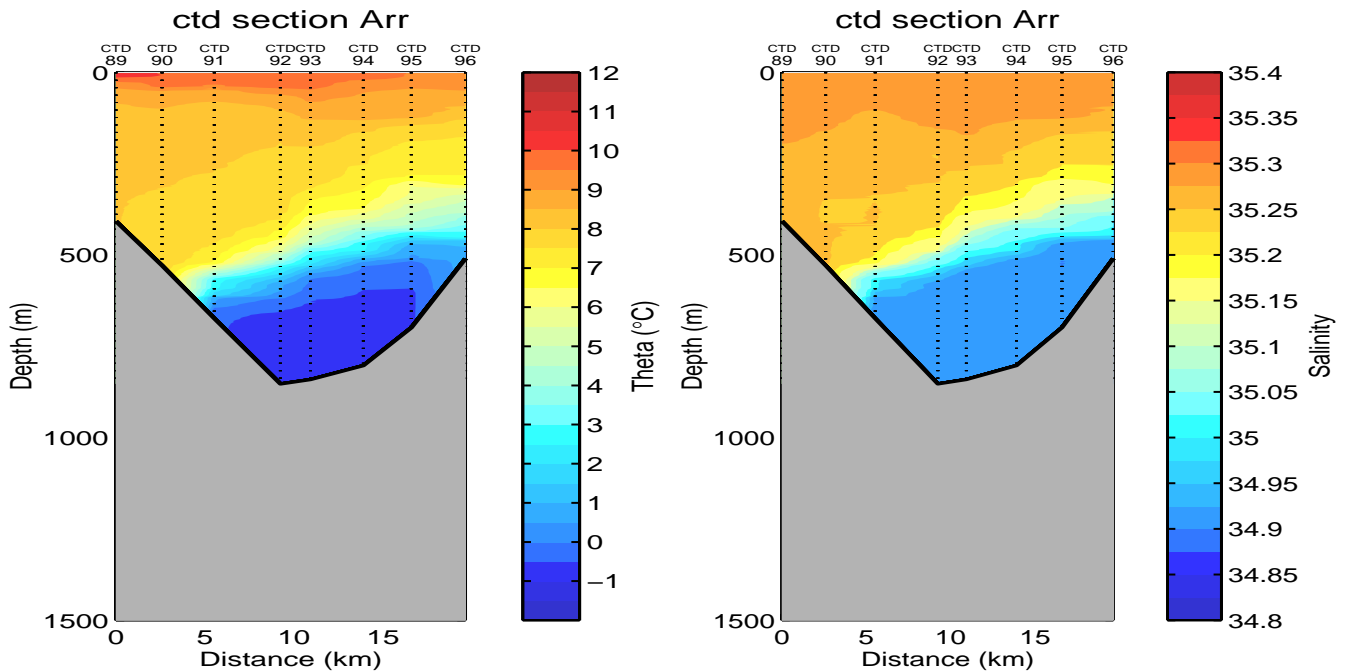


Figure 11: A section of potential temperature (left) and salinity (right) made up from CTD stations taken across the narrow part of the Faroe Bank Channel overflow (see Figure 6 for details of station locations). This view is to the west and in the direction of the overflow current.

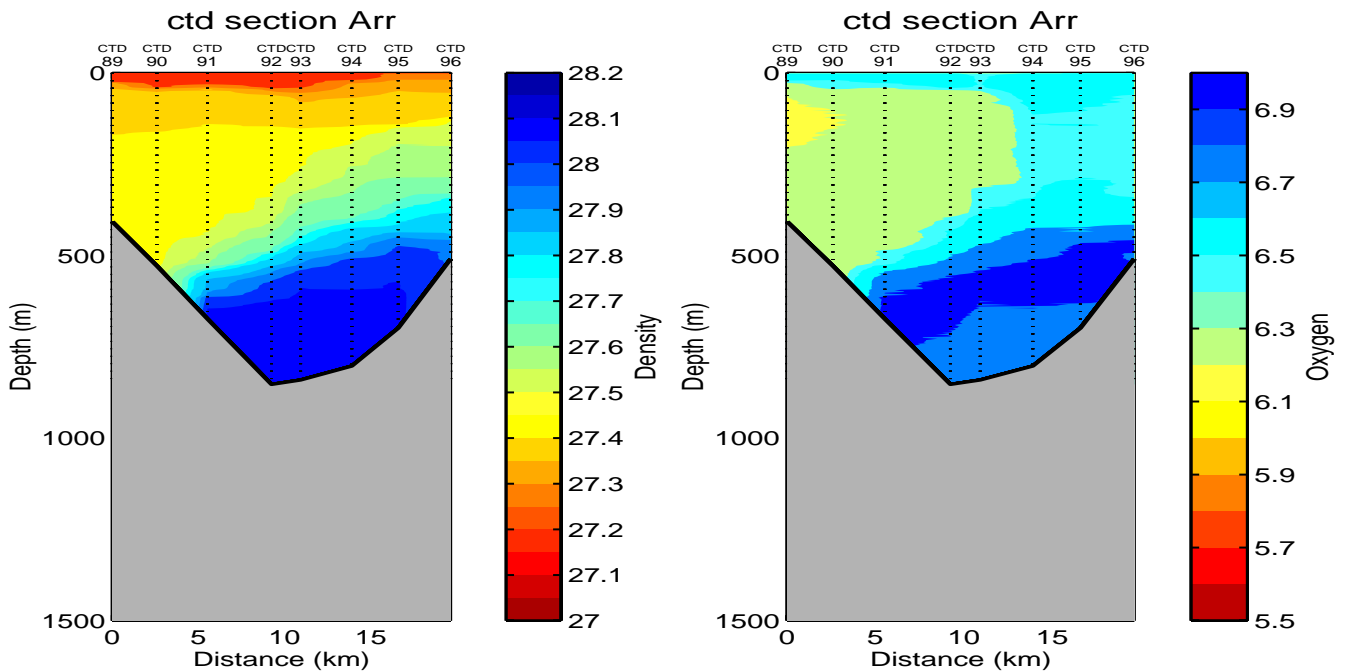


Figure 12: A section of potential density (left) and oxygen concentration (right) made up from CTD stations taken across the narrow part of the Faroe Bank Channel overflow (see Figure 6 for details of station locations). This view is to the west, or in the direction of the overflow current.

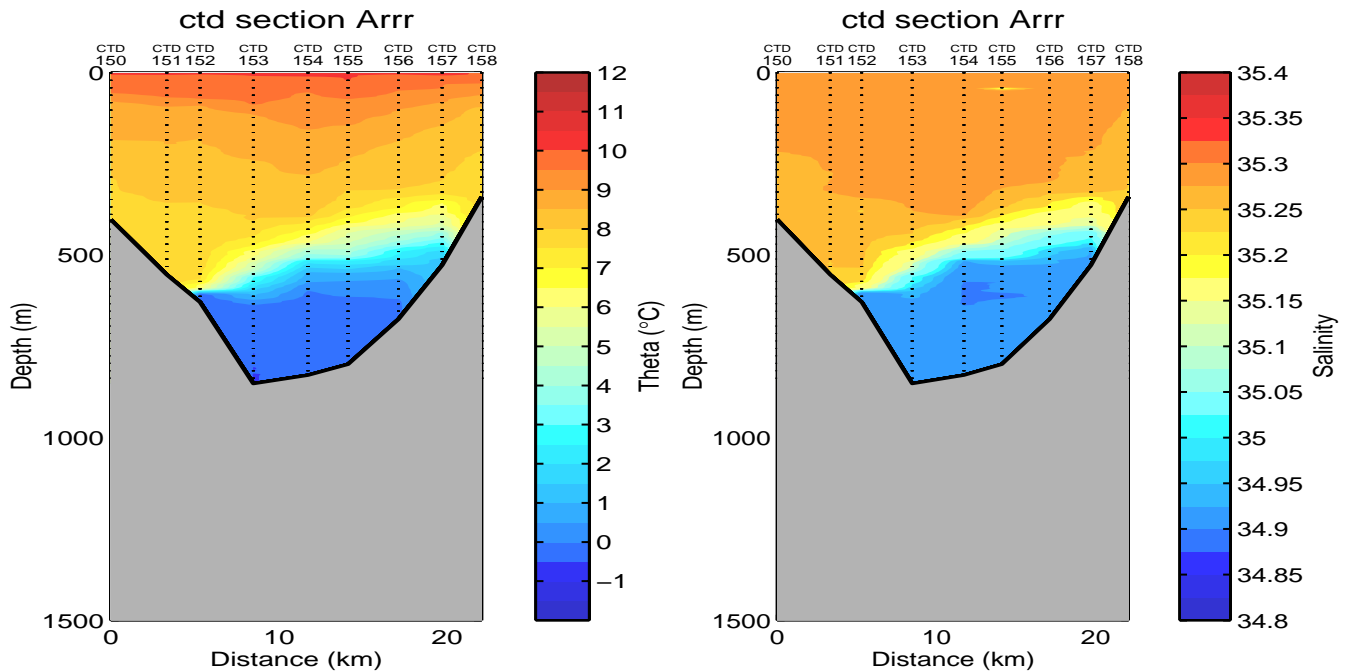


Figure 13: A section of potential temperature (left) and salinity (right) made up from CTD stations taken across the narrow part of the Faroe Bank Channel overflow (see Figure 6 for details of station locations). This view is to the west and in the direction of the overflow current.

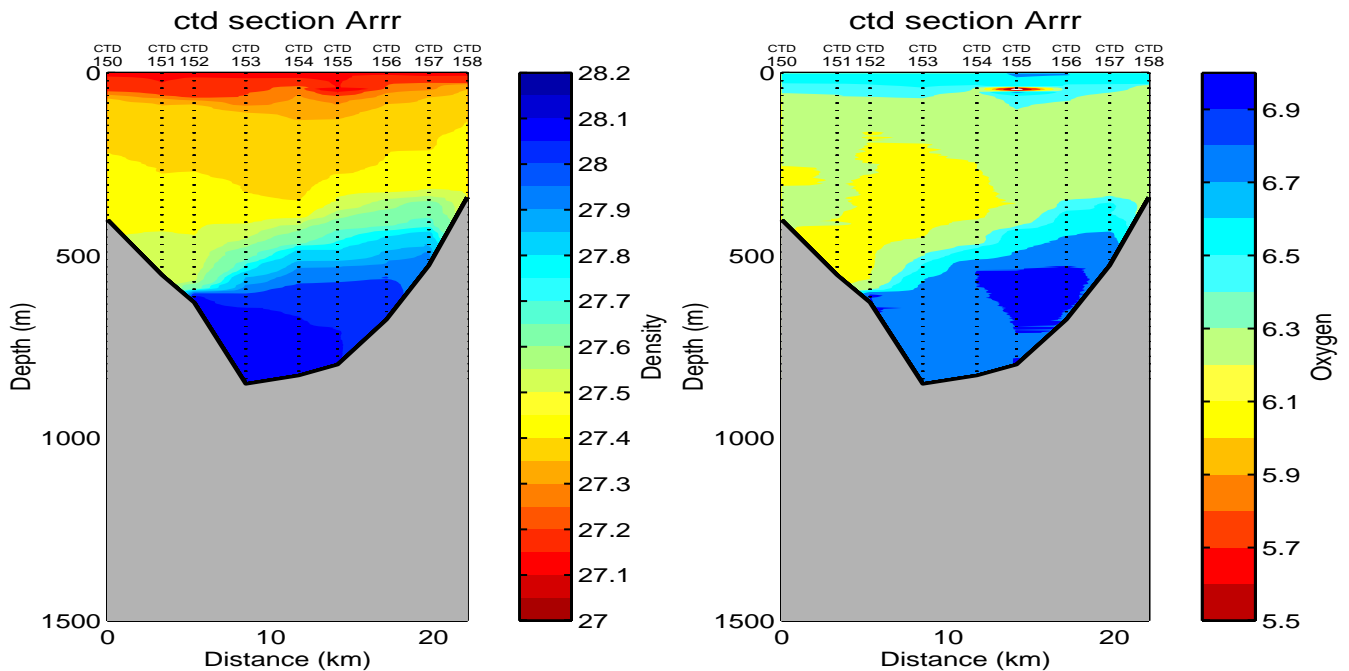


Figure 14: A section of potential density (left) and oxygen concentration (right) made up from CTD stations taken across the narrow part of the Faroe Bank Channel overflow (see Figure 6 for details of station locations). This view is to the west, or in the direction of the overflow current.

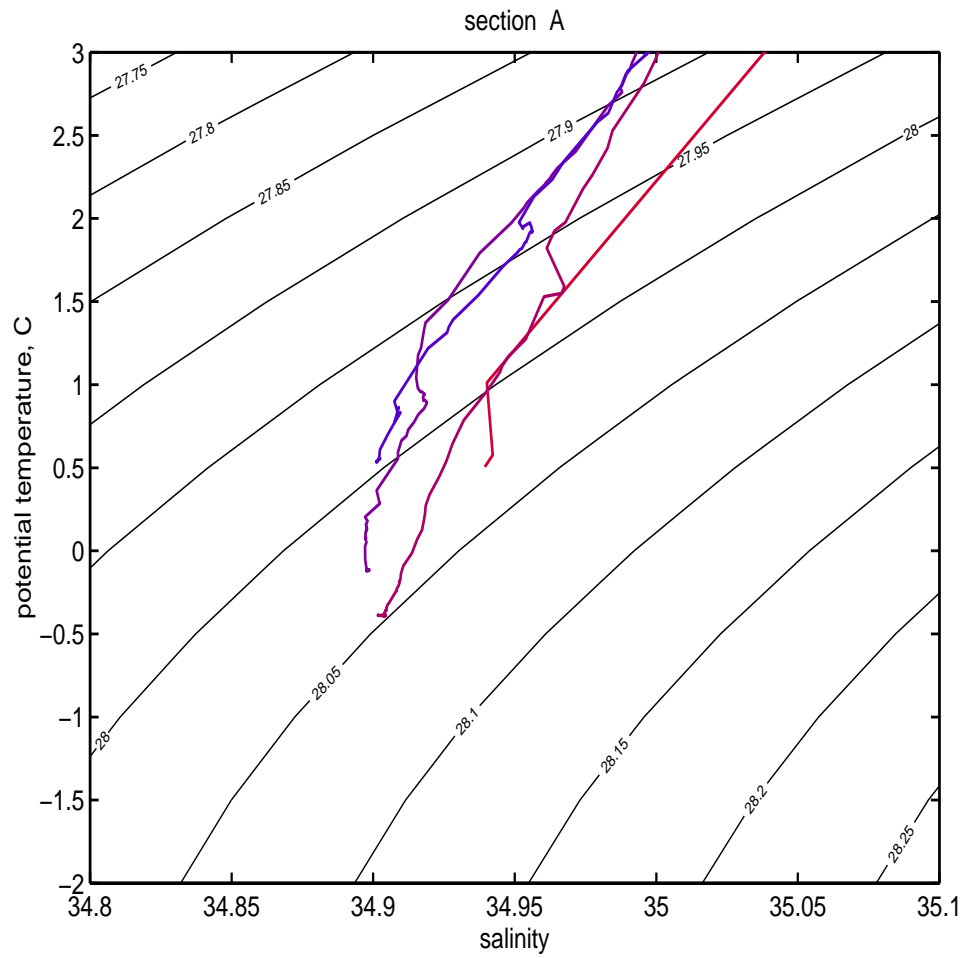


Figure 15: T-S diagram from section A. The colors indicate profiles made from south (red) to north (to blue).

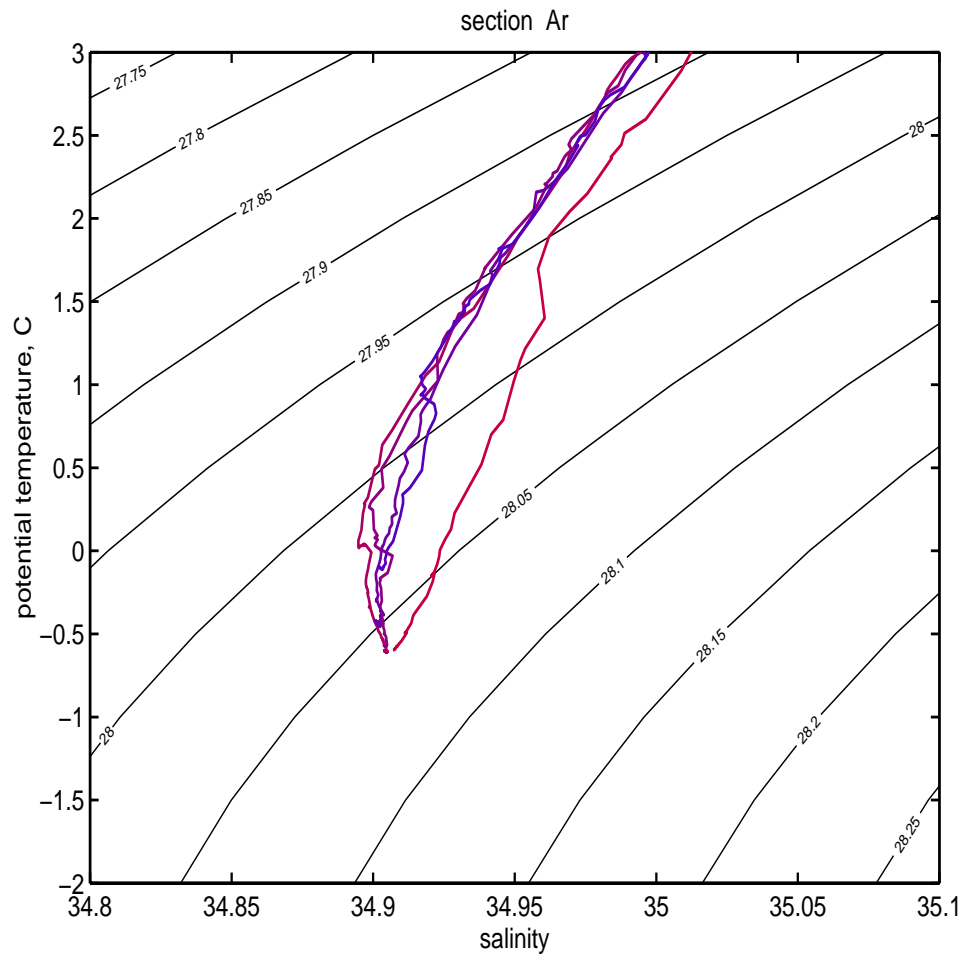


Figure 16: T-S diagram from section Ar. The colors indicate profiles made from south (red) to north (to blue).

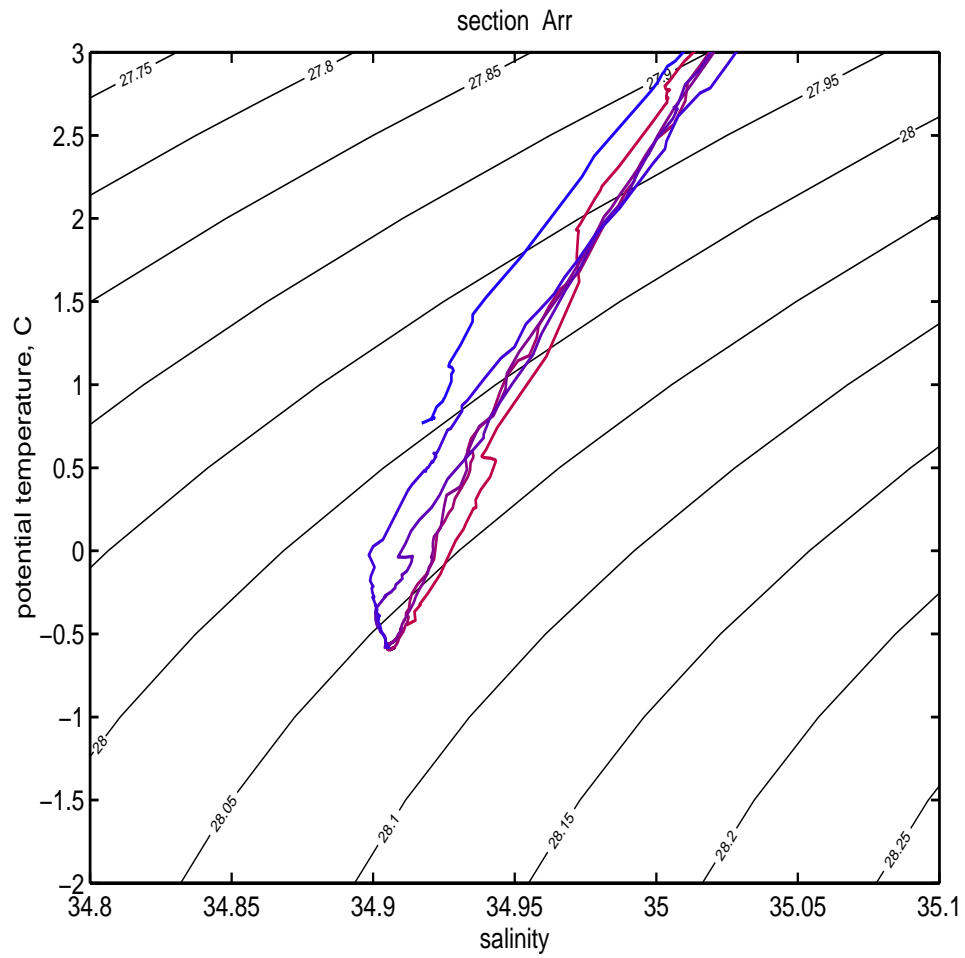


Figure 17: T-S diagram from section Arr. The colors indicate profiles made from south (red) to north (to blue) and the contours are of potential density.

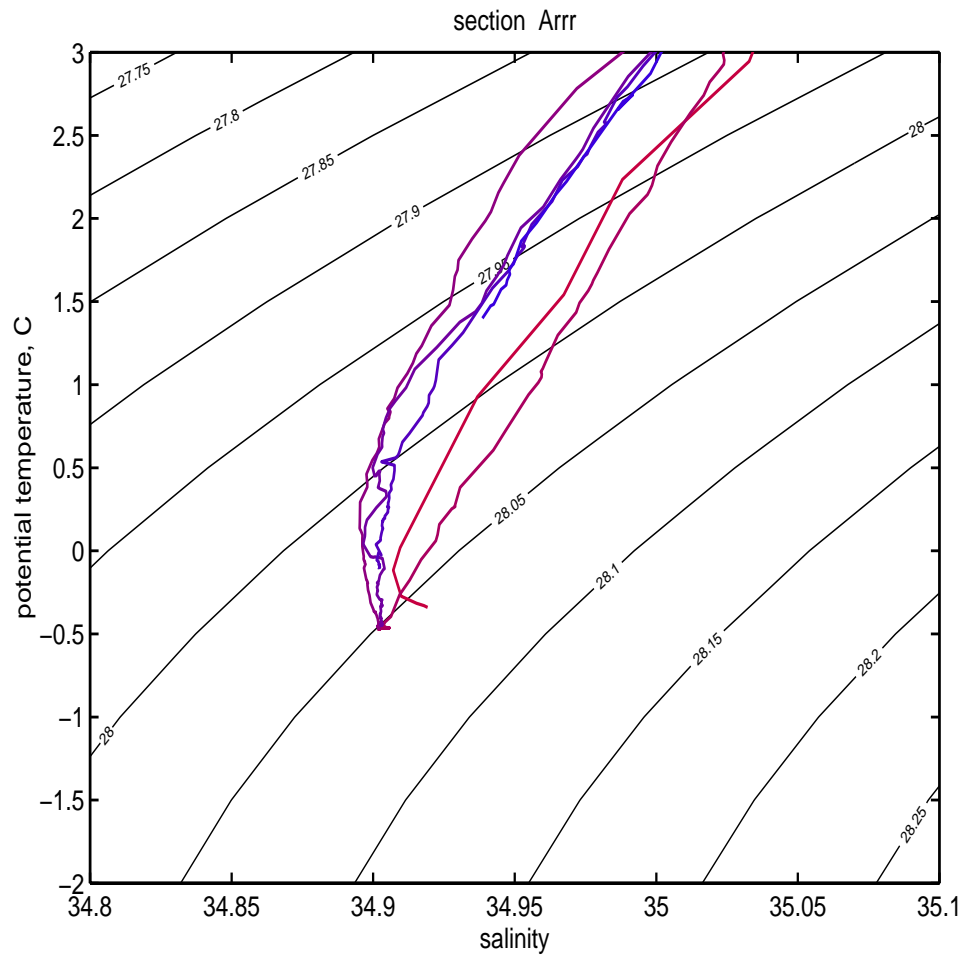


Figure 18: T-S diagram from section Arrr. The colors indicate profiles made from south (red) to north (to blue).

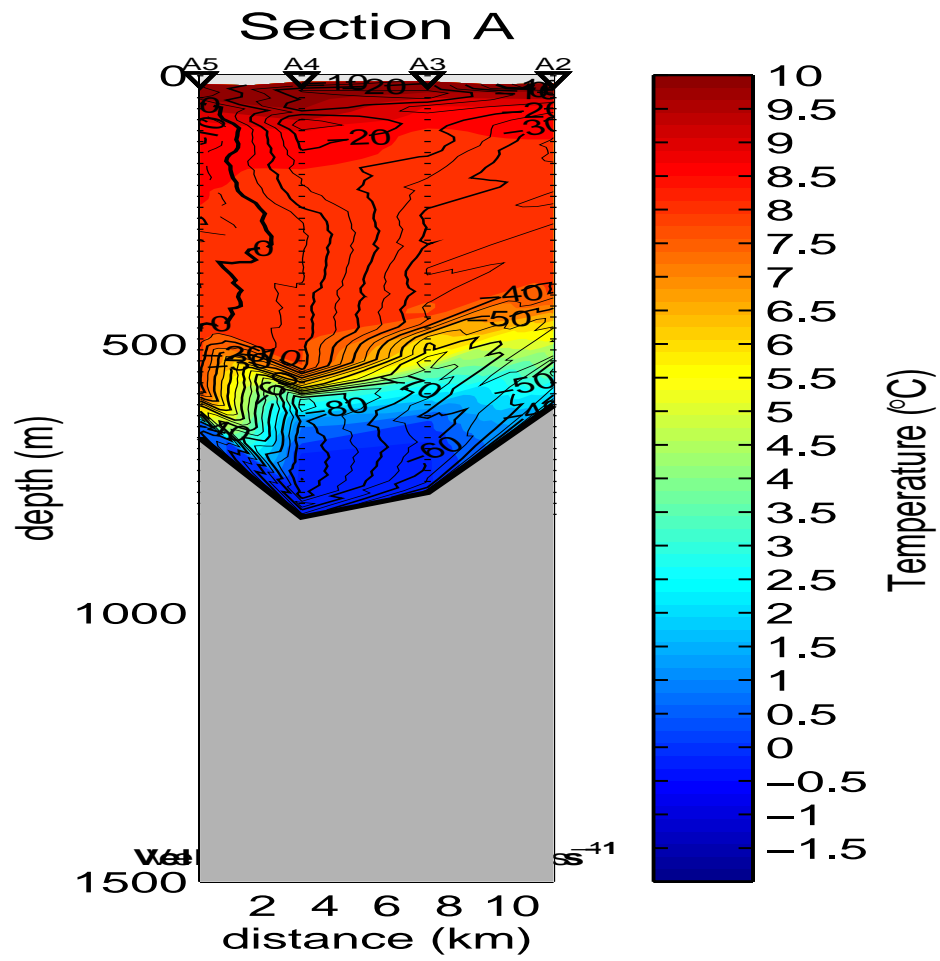


Figure 19: XCP-measured temperature (color coded) and current component normal to the section (contoured, units are  $\text{cm s}^{-1}$ ) on section A.

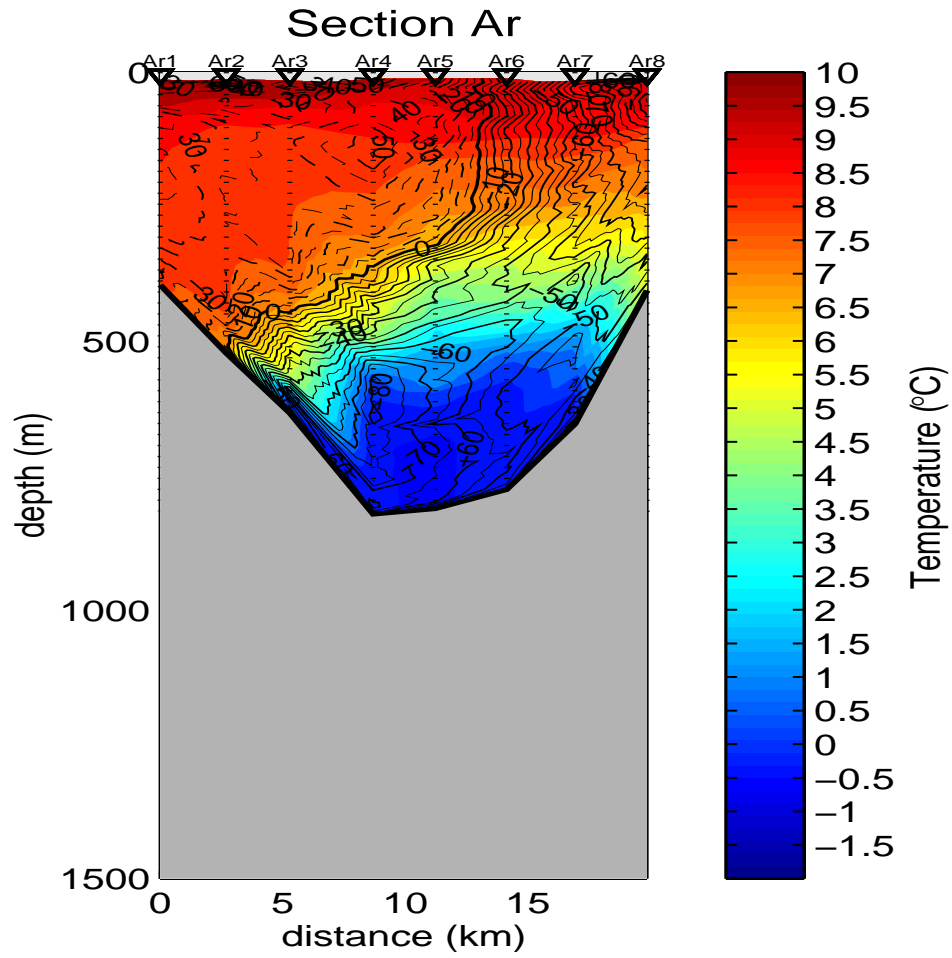


Figure 20: XCP-measured temperature (color coded) and current component normal to the section (contoured, units are  $\text{cm s}^{-1}$ ) on section Ar.

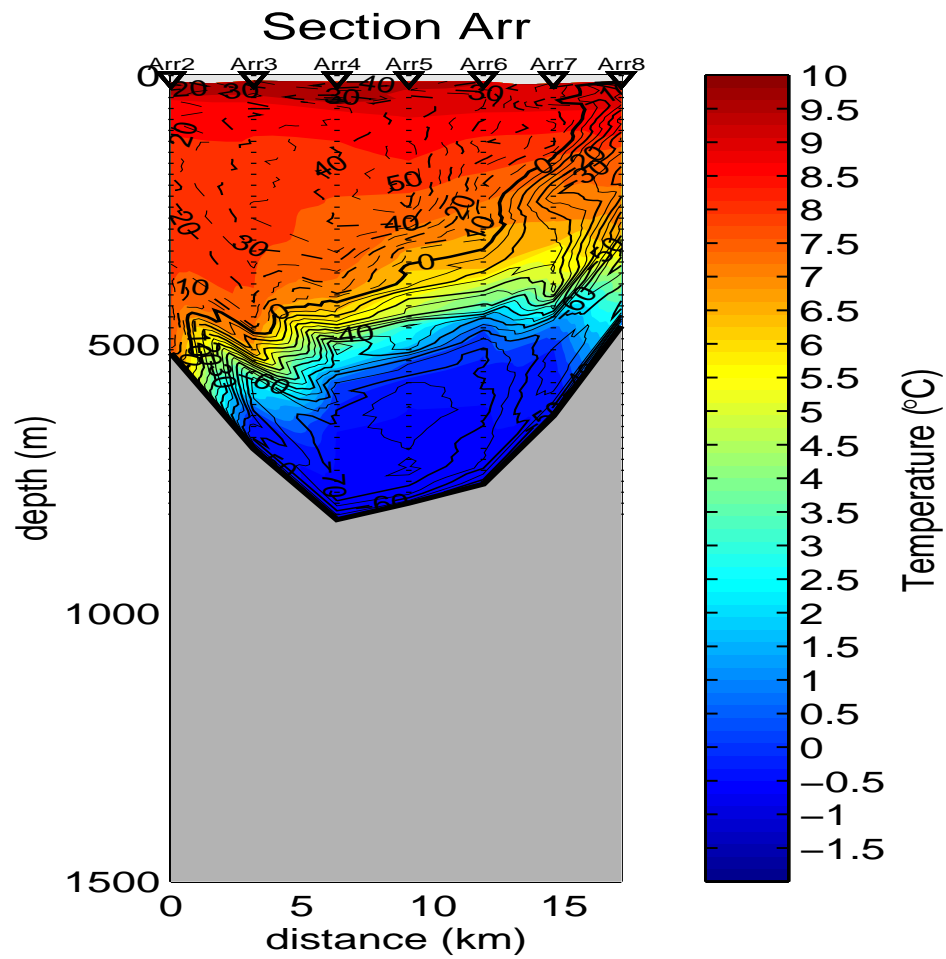


Figure 21: XCP-measured temperature (color coded) and current component normal to the section (contoured, units are  $\text{cm s}^{-1}$ ) on section Arr.

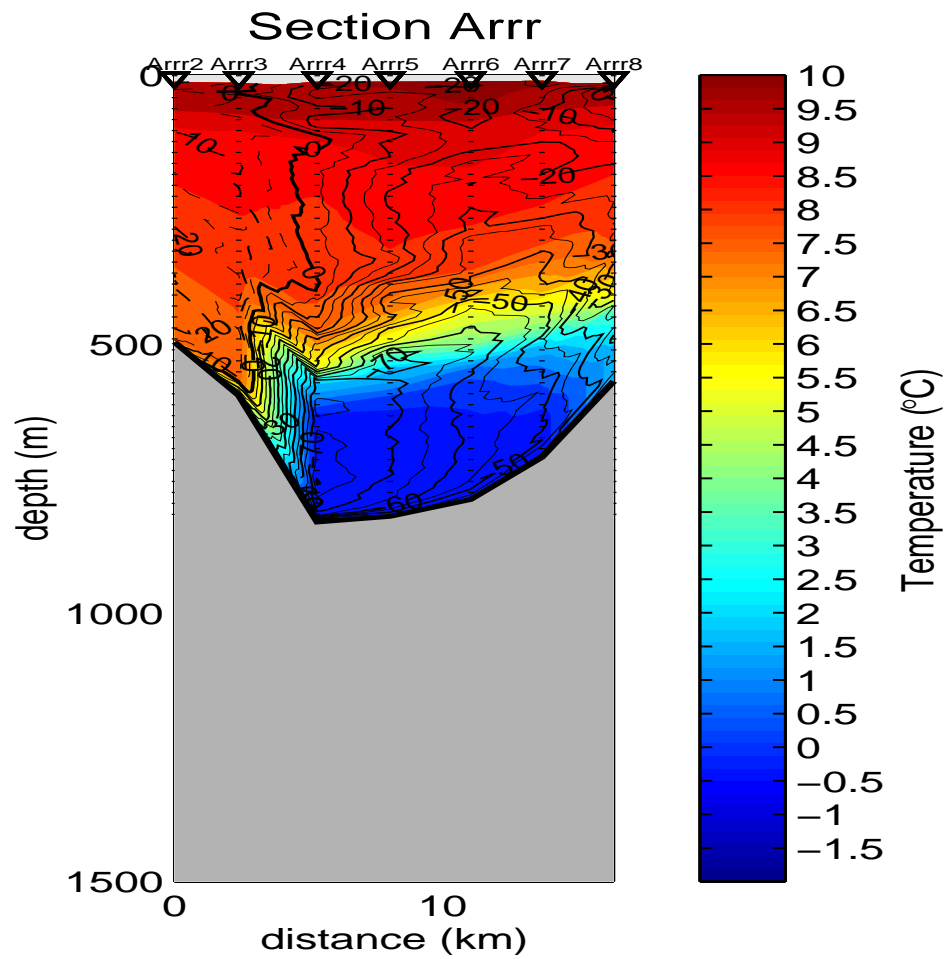


Figure 22: XCP-measured temperature (color coded) and current component normal to the section (contoured, units are  $\text{cm s}^{-1}$ ) on section Arrr.

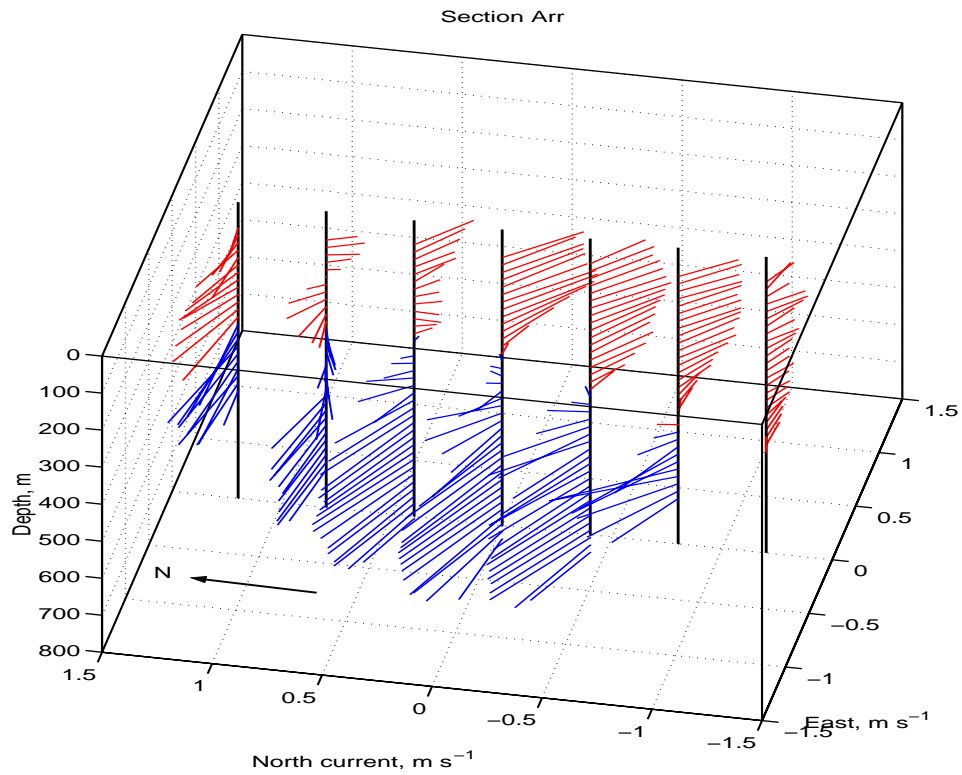


Figure 23: Currents measured by XCPs across a narrow section (section Arr) of the Faroe Bank Channel. In the current diagram, the view is toward the east, and currents with temperature less than 7 C are shown in blue (the overflow water that flows west-northwestward at this section). The shallower currents are mainly eastward flowing and comparatively warm North Atlantic water (temperatures greater than 7 C are red vectors).

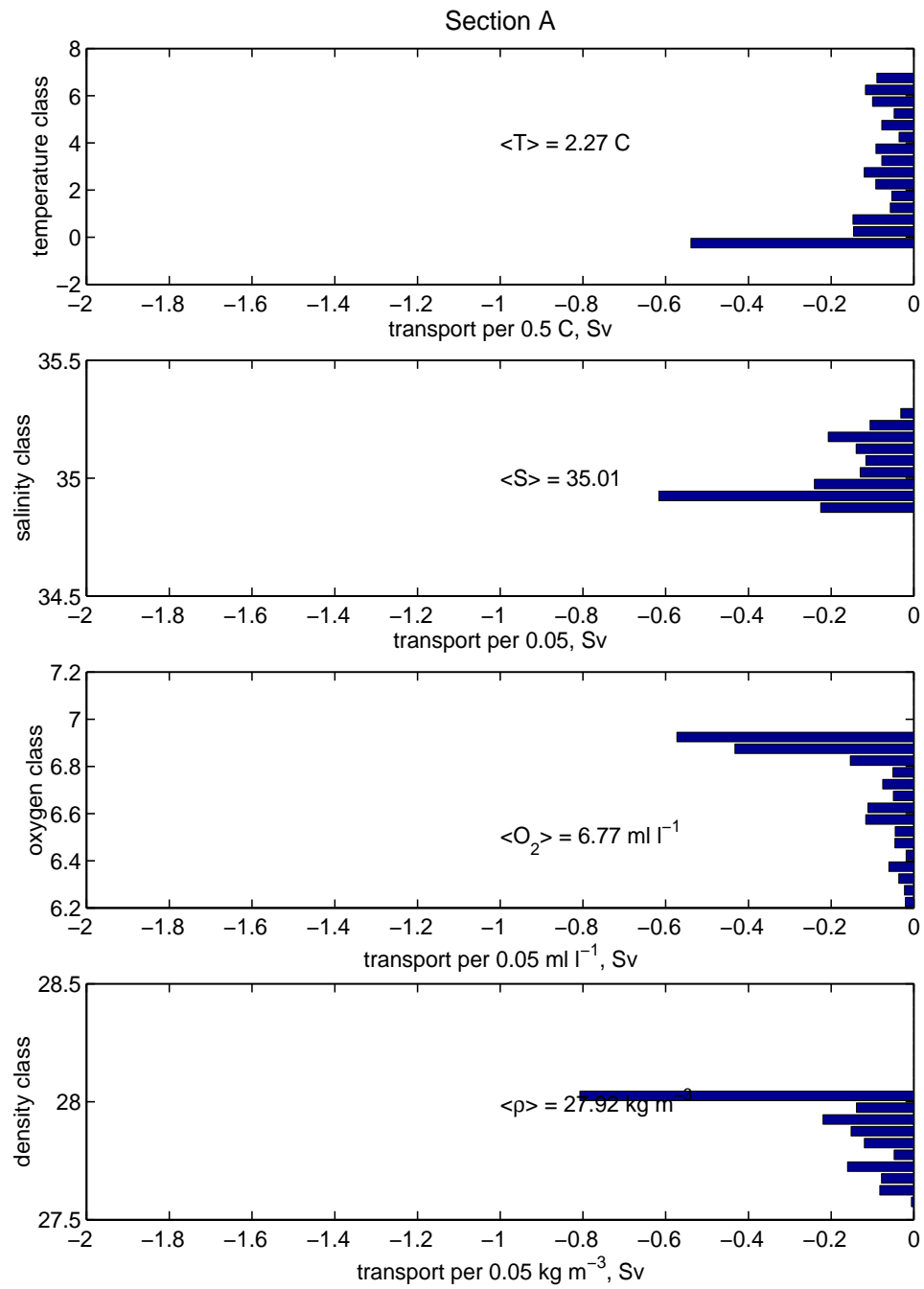


Figure 24: Transport of temperature, salinity, density and oxygen shown in variable classes across section A. Currents were measured by XCP and hydrographic variables by CTD.

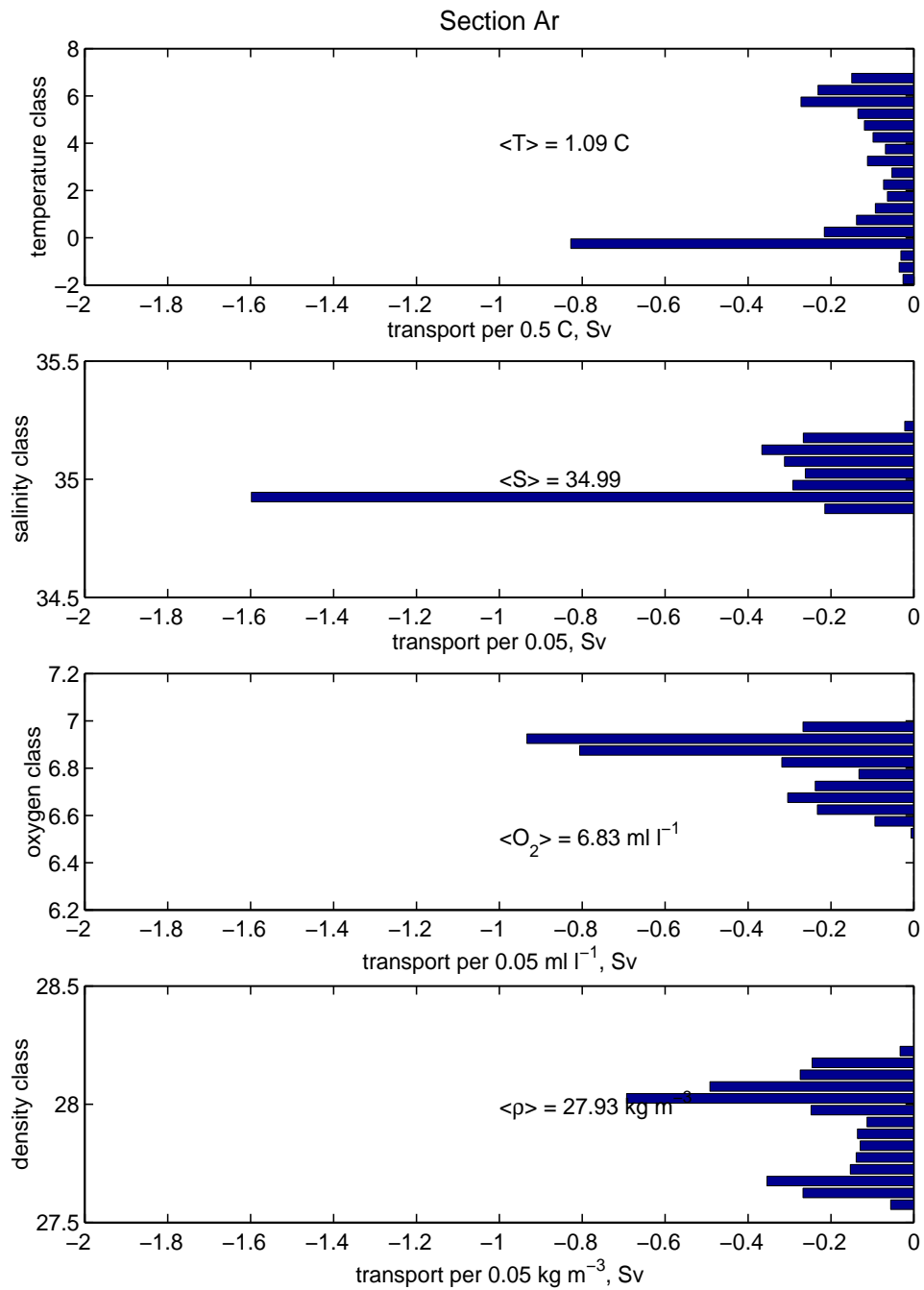


Figure 25: Transport of temperature, salinity, density and oxygen shown in variable classes across section Ar. Currents were measured by XCP and hydrographic variables by CTD.

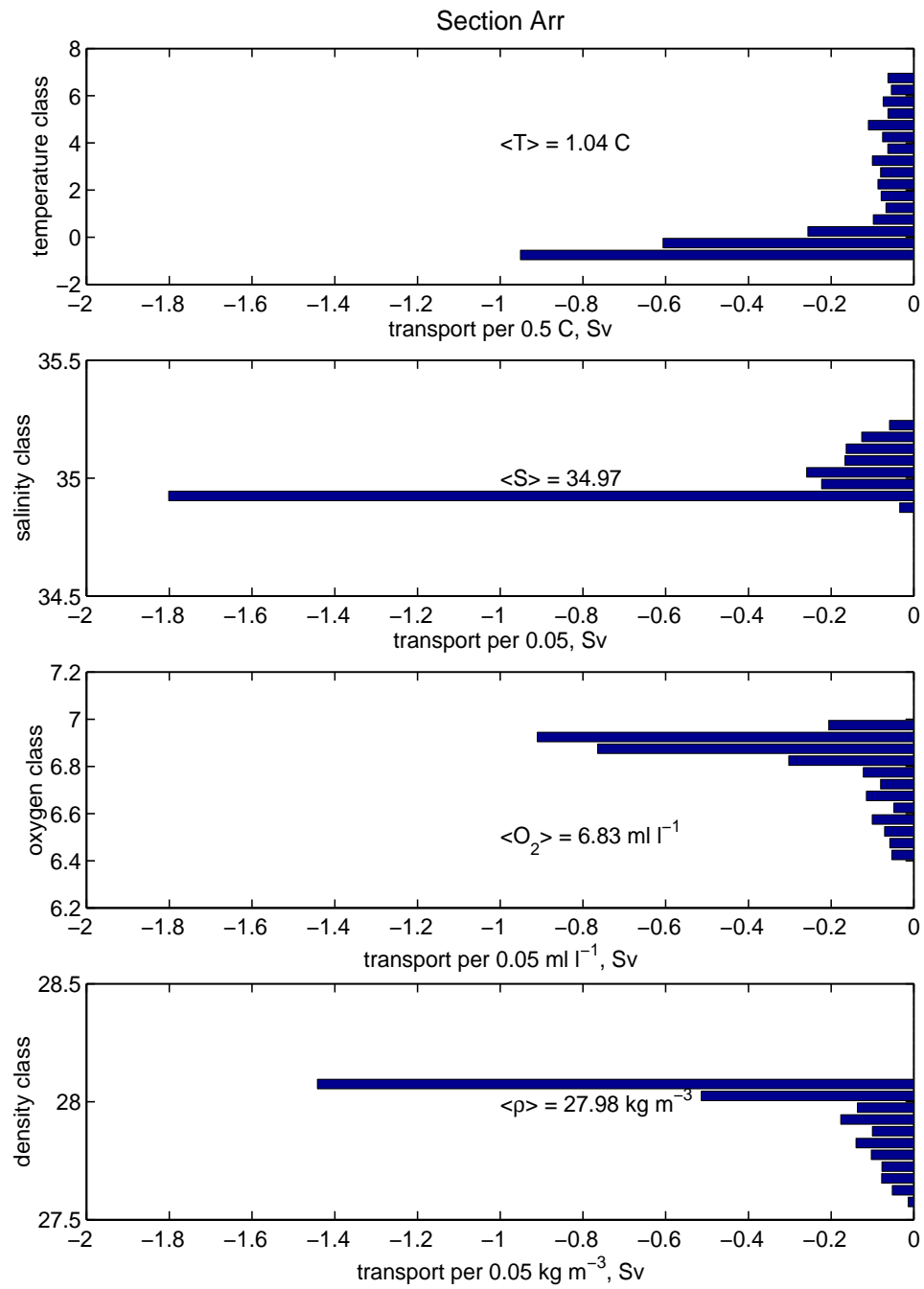


Figure 26: Transport of temperature, salinity, density and oxygen shown in variable classes across section Arr. Currents were measured by XCP and hydrographic variables by CTD.

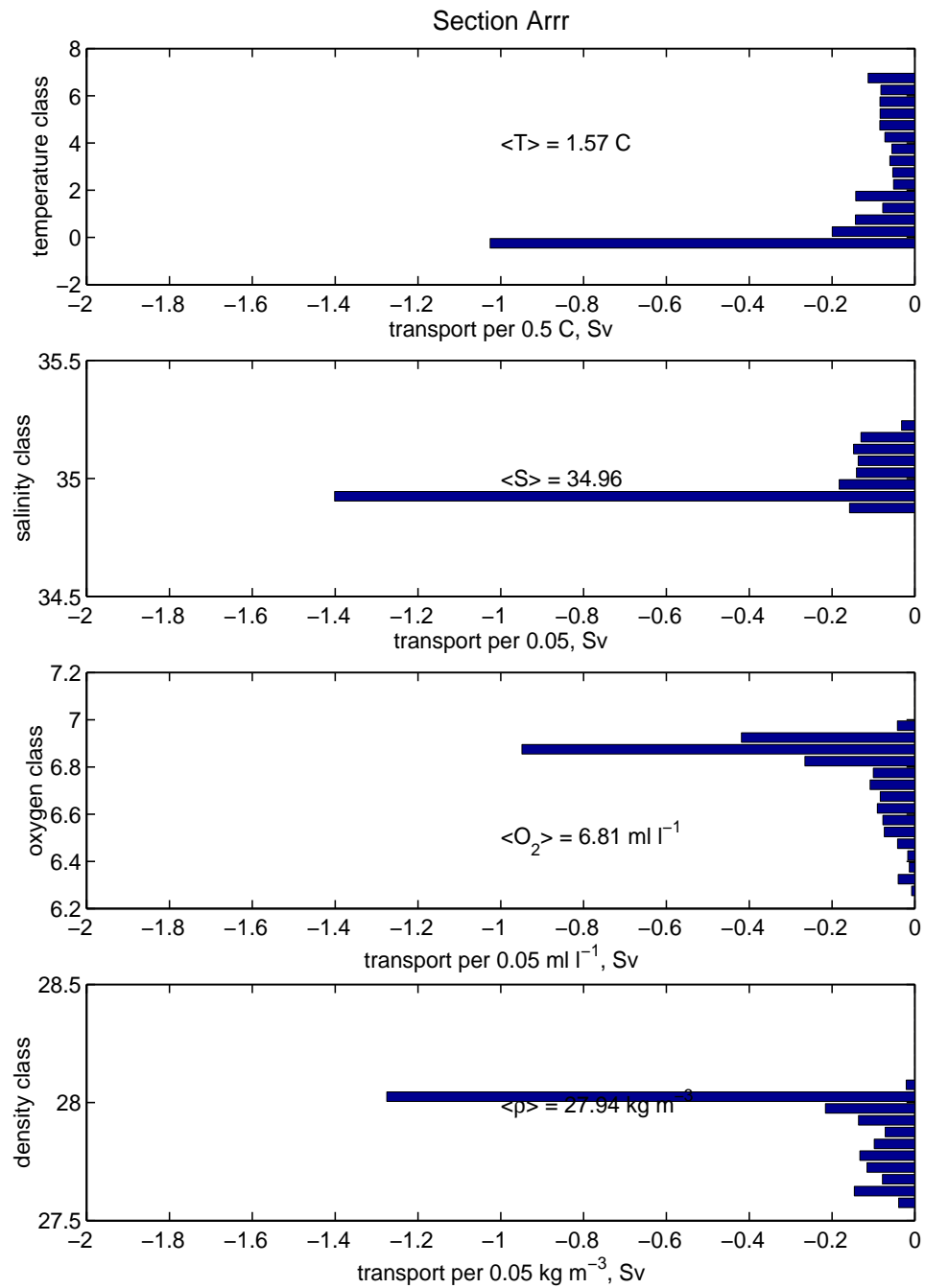


Figure 27: Transport of temperature, salinity, density and oxygen shown in variable classes across section Arrr. Currents were measured by XCP and hydrographic variables by CTD.

## 7 Other, Selected CTD and XCP Sections

A few other sections are shown next. These comprise about one third of the remaining section data. The other sections may be found on the web site.

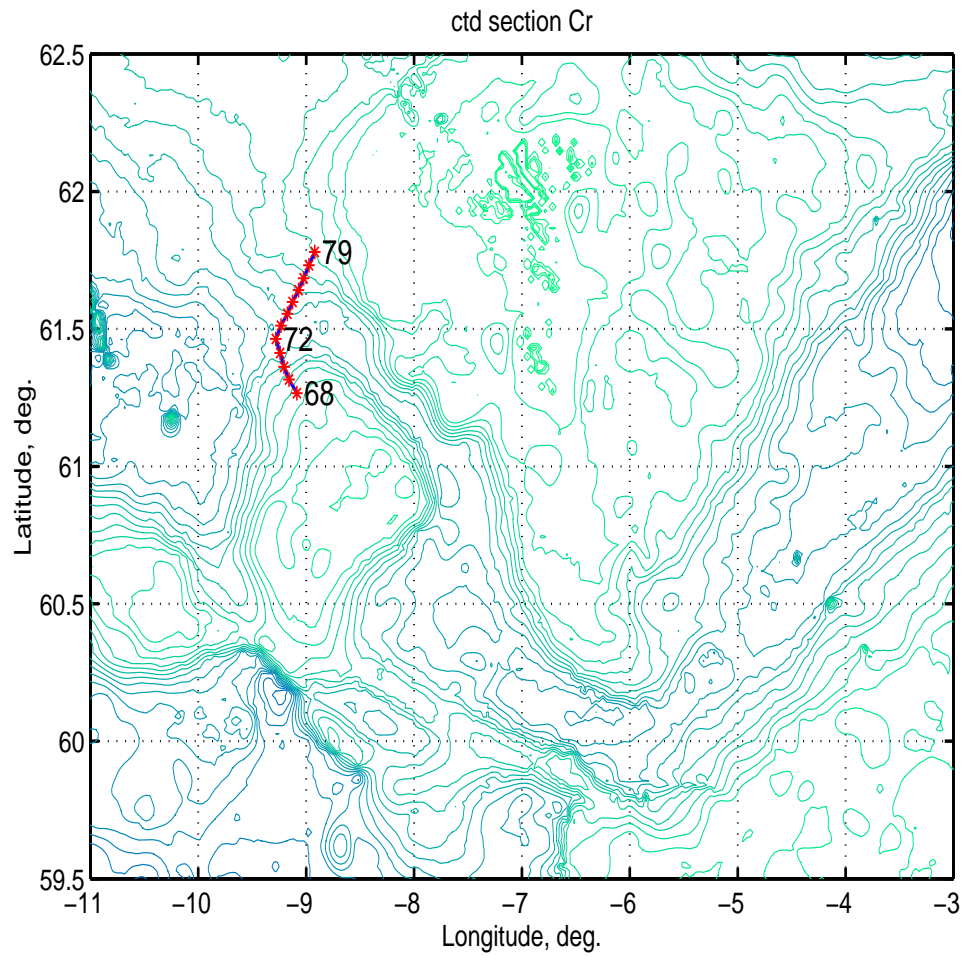


Figure 28: Station locations for section Cr.

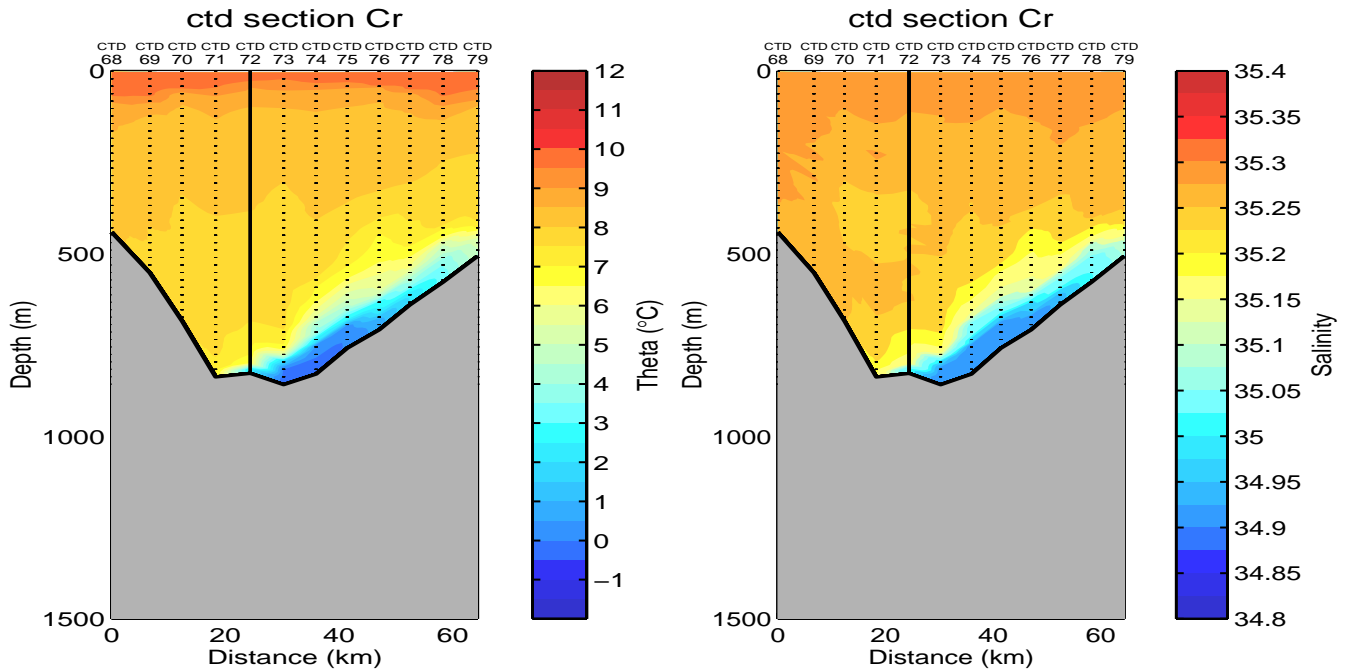


Figure 29: A section of potential temperature (left) and salinity (right) made up from CTD stations taken across the Faroe Bank Channel overflow just to the west of the narrow channel. (see Figure 28 for details of station locations). This view is to the west and in the direction of the overflow current.

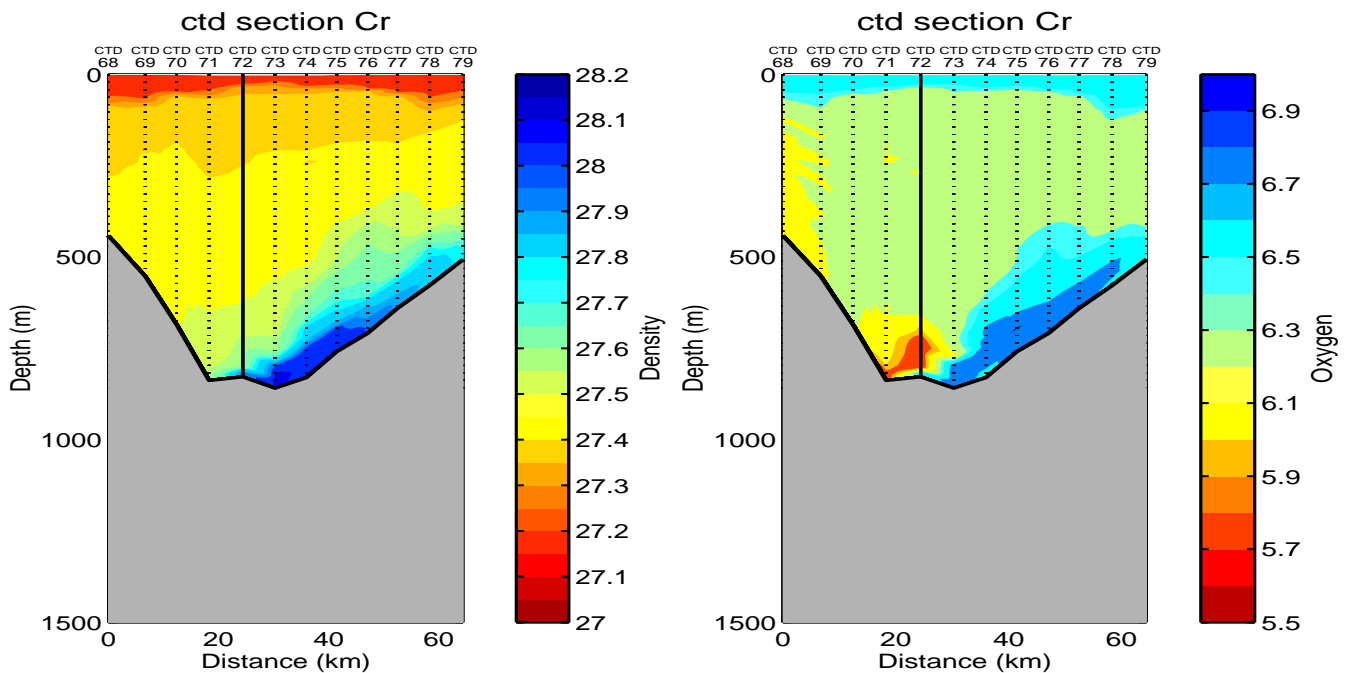


Figure 30: A section of potential density (left) and oxygen (right) made up from CTD stations taken across the Faroe Bank Channel overflow just to the west of the narrow channel. (see Figure 28 for details of station locations). This view is to the west, or in the direction of the overflow current.

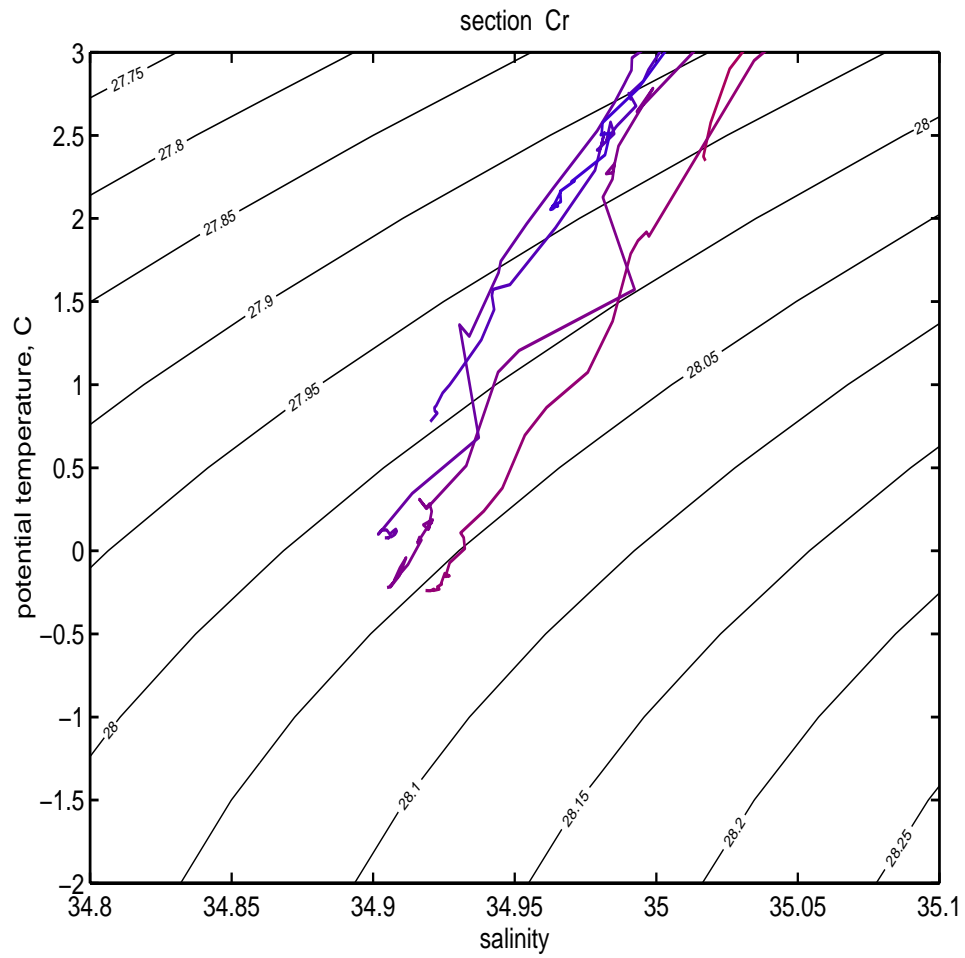


Figure 31: T-S diagram from section Crr. The colors indicate profiles made from south (red) to north (to blue).

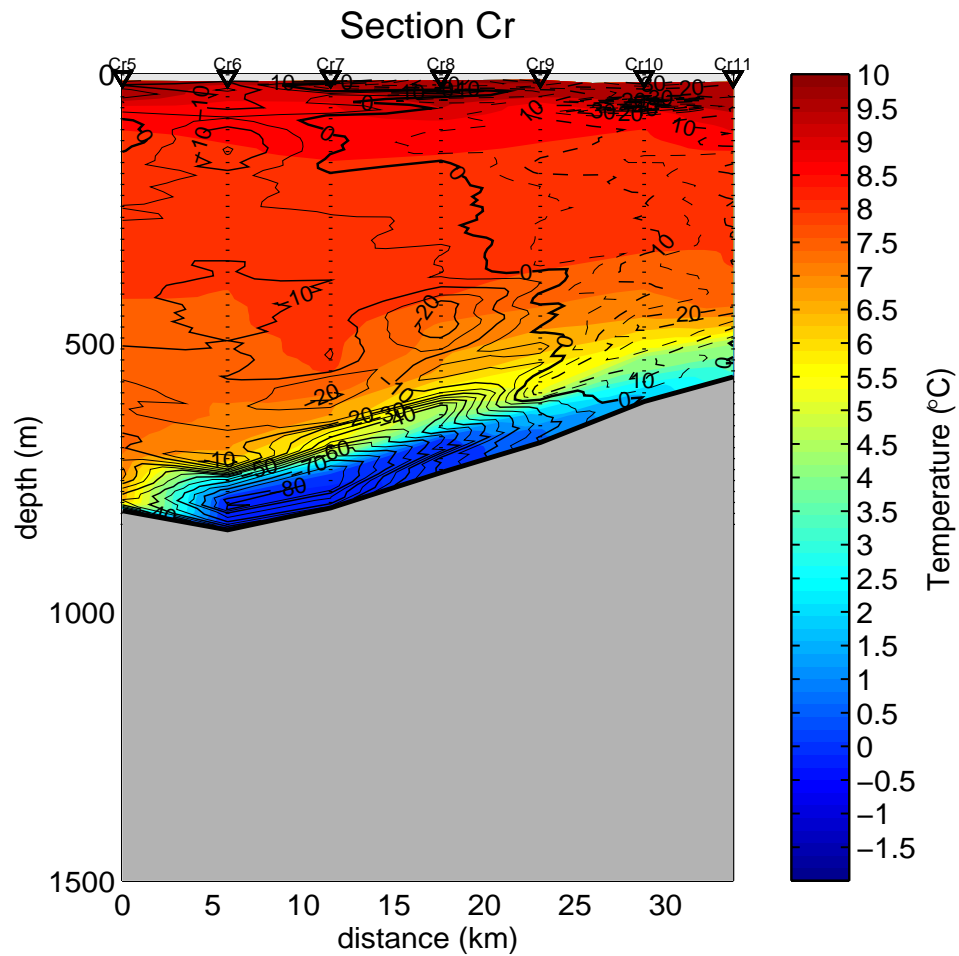


Figure 32: XCP-measured temperature (color coded) and current component normal to the section (contoured, units are  $\text{cm s}^{-1}$ ) on section Cr.

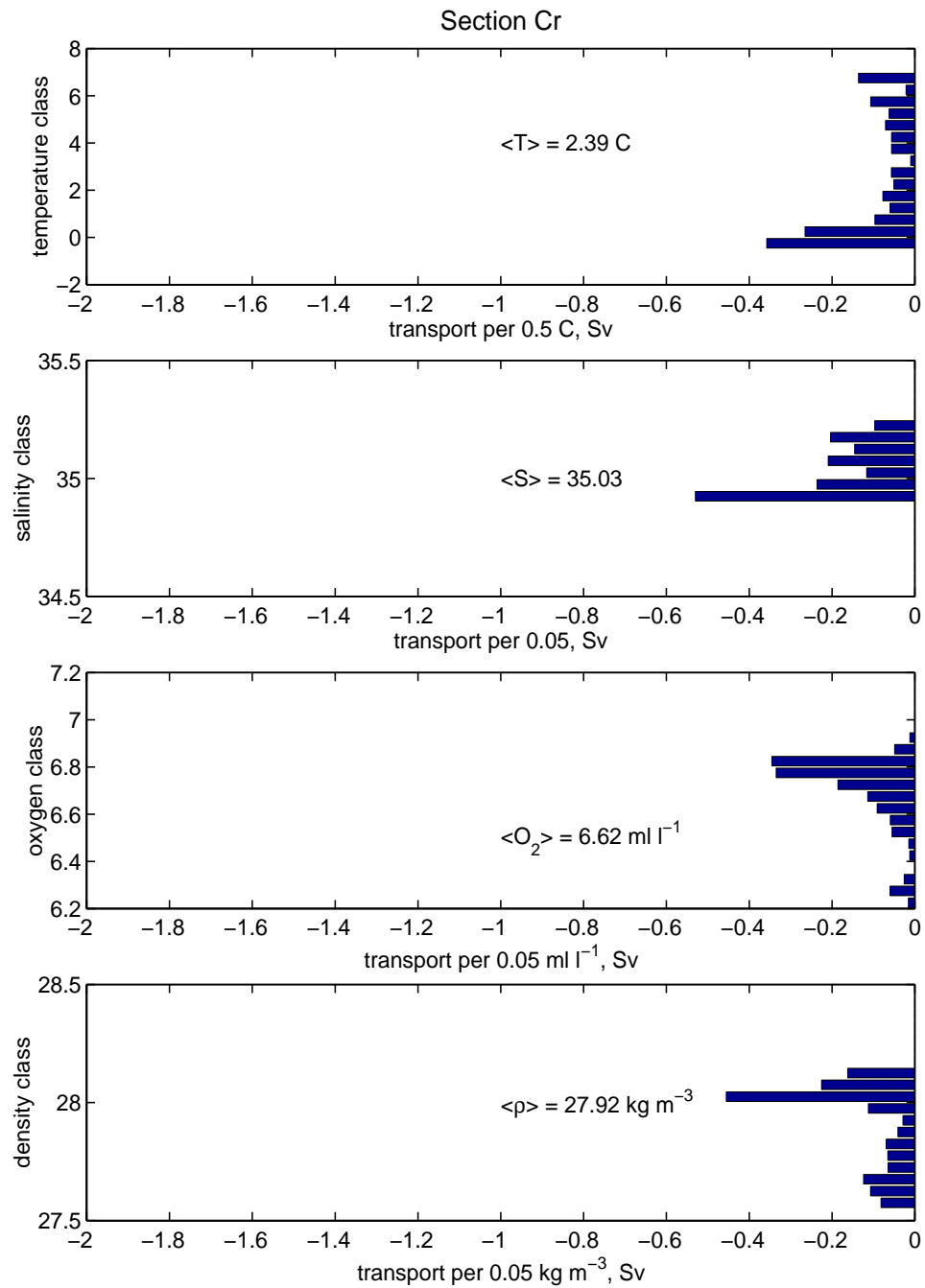


Figure 33: Transport of temperature, salinity, density and oxygen shown in variable classes across section Crr. Currents were measured by XCP and hydrographic variables by CTD.

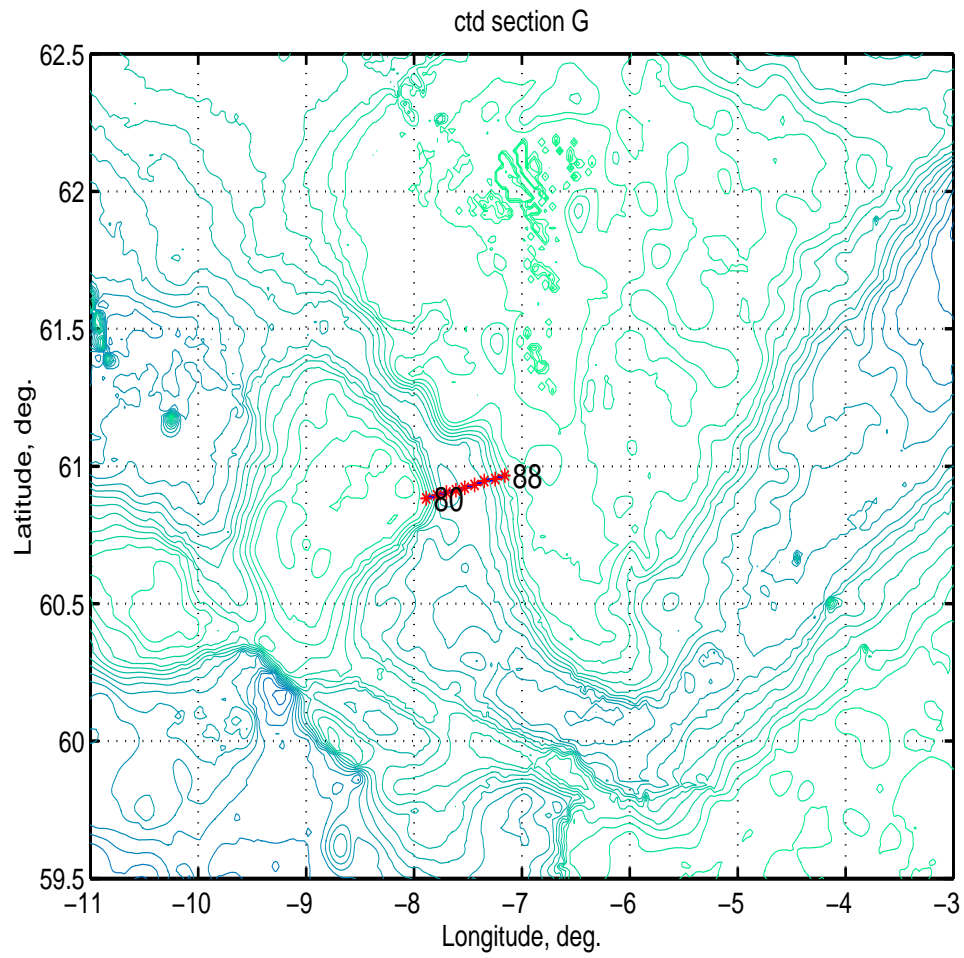


Figure 34: Station locations for section G.

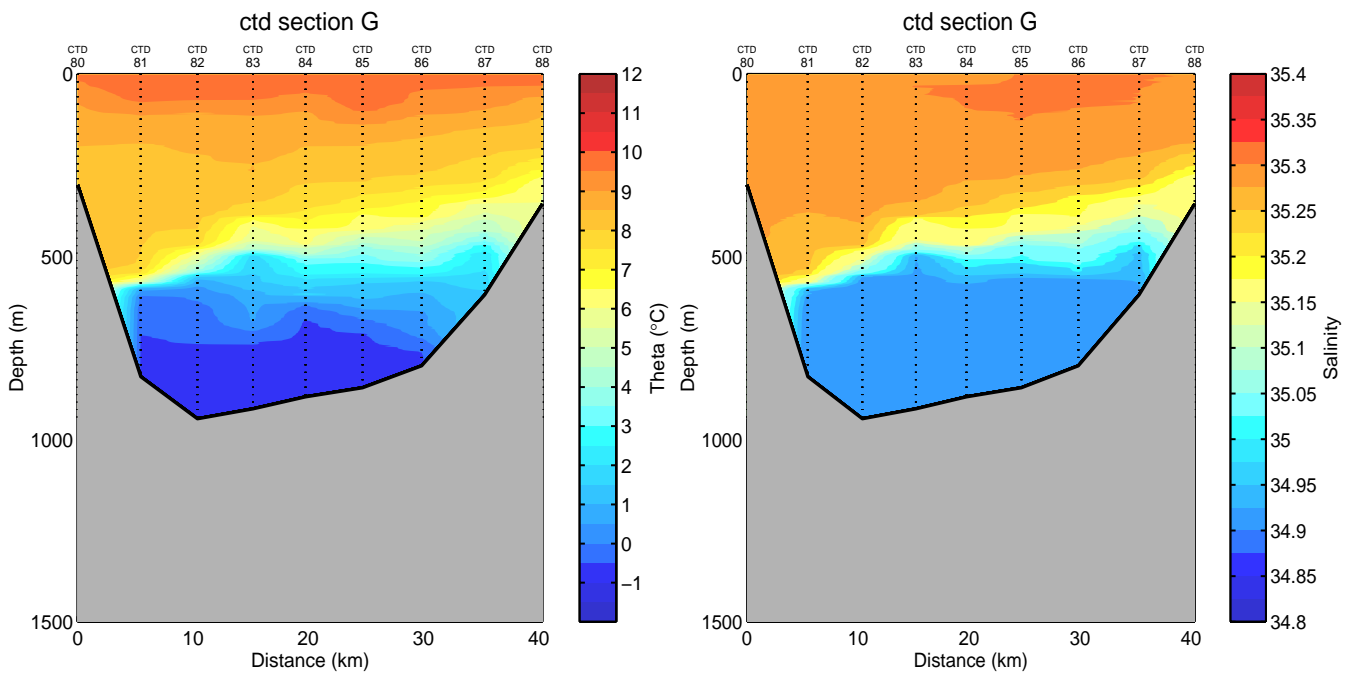


Figure 35: A section of potential temperature (left) and salinity (right) made up from CTD stations taken across the Faroe Bank Channel overflow just to the east of the narrow channel. (see Figure 34 for details of station locations). This view is to the west and in the direction of the overflow current.

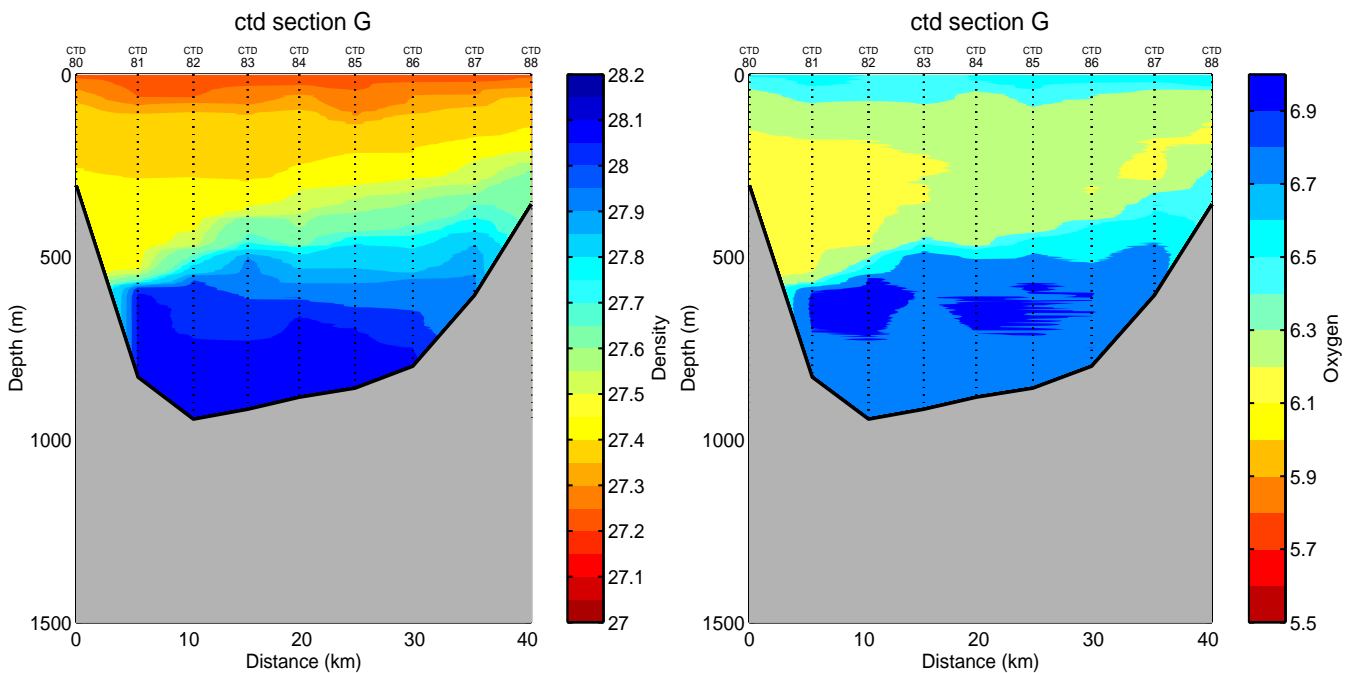


Figure 36: A section of potential density (left) and oxygen (right) made up from CTD stations taken across the Faroe Bank Channel overflow just to the east of the narrow channel. (see Figure 34 for details of station locations). This view is to the west, or in the direction of the overflow current.

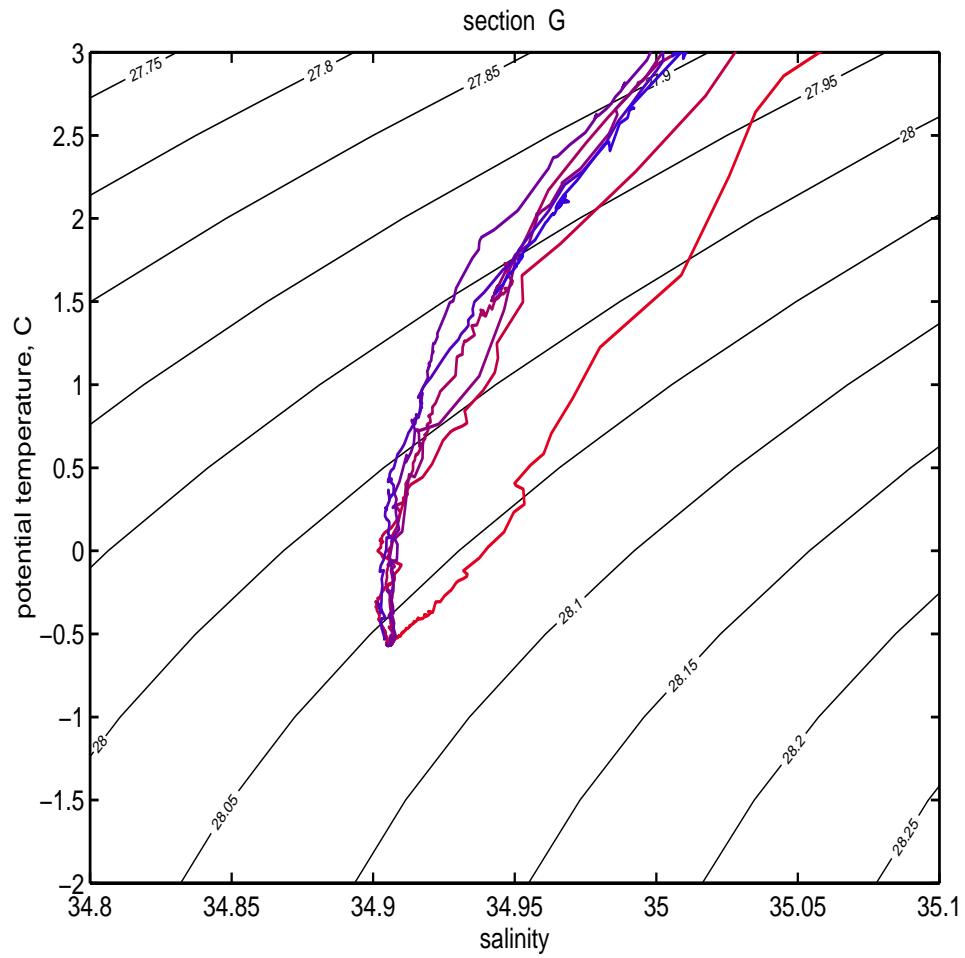


Figure 37: T-S diagram from section G. The colors indicate profiles made from south (red) to north (to blue).

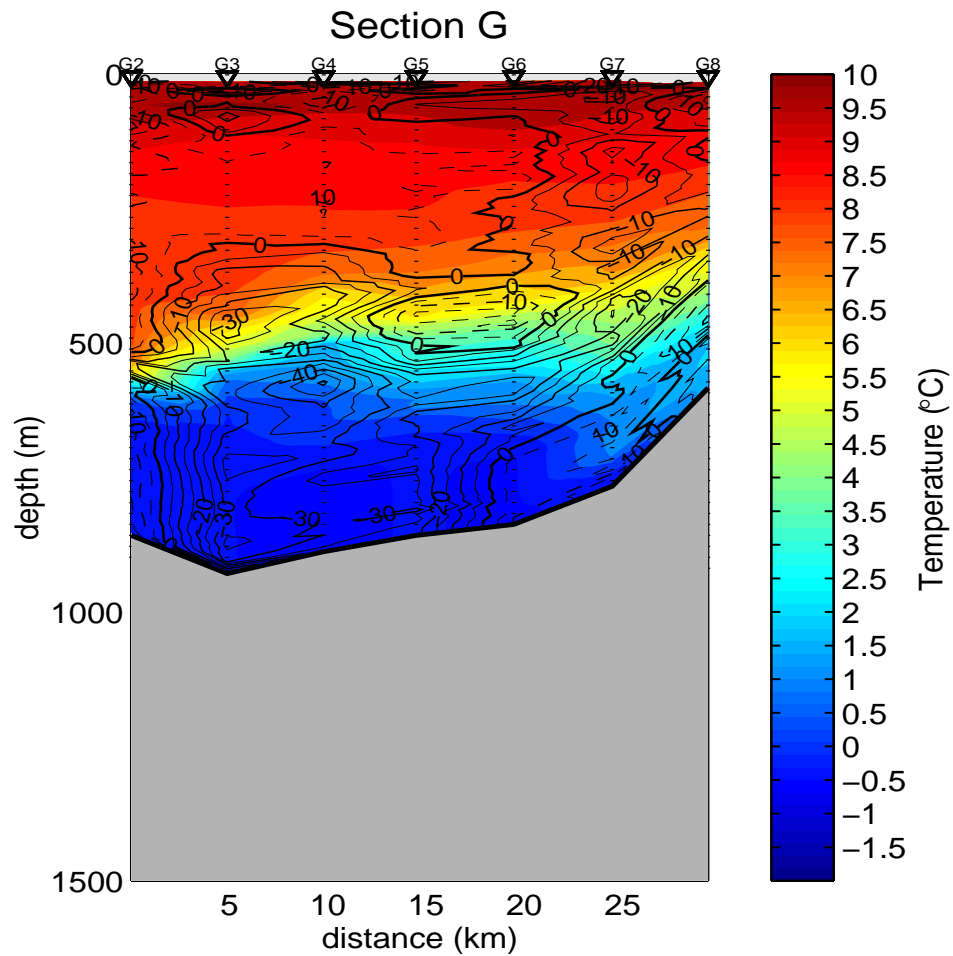


Figure 38: XCP-measured temperature (color coded) and current component normal to the section (contoured, units are  $\text{cm s}^{-1}$ ) on section G.

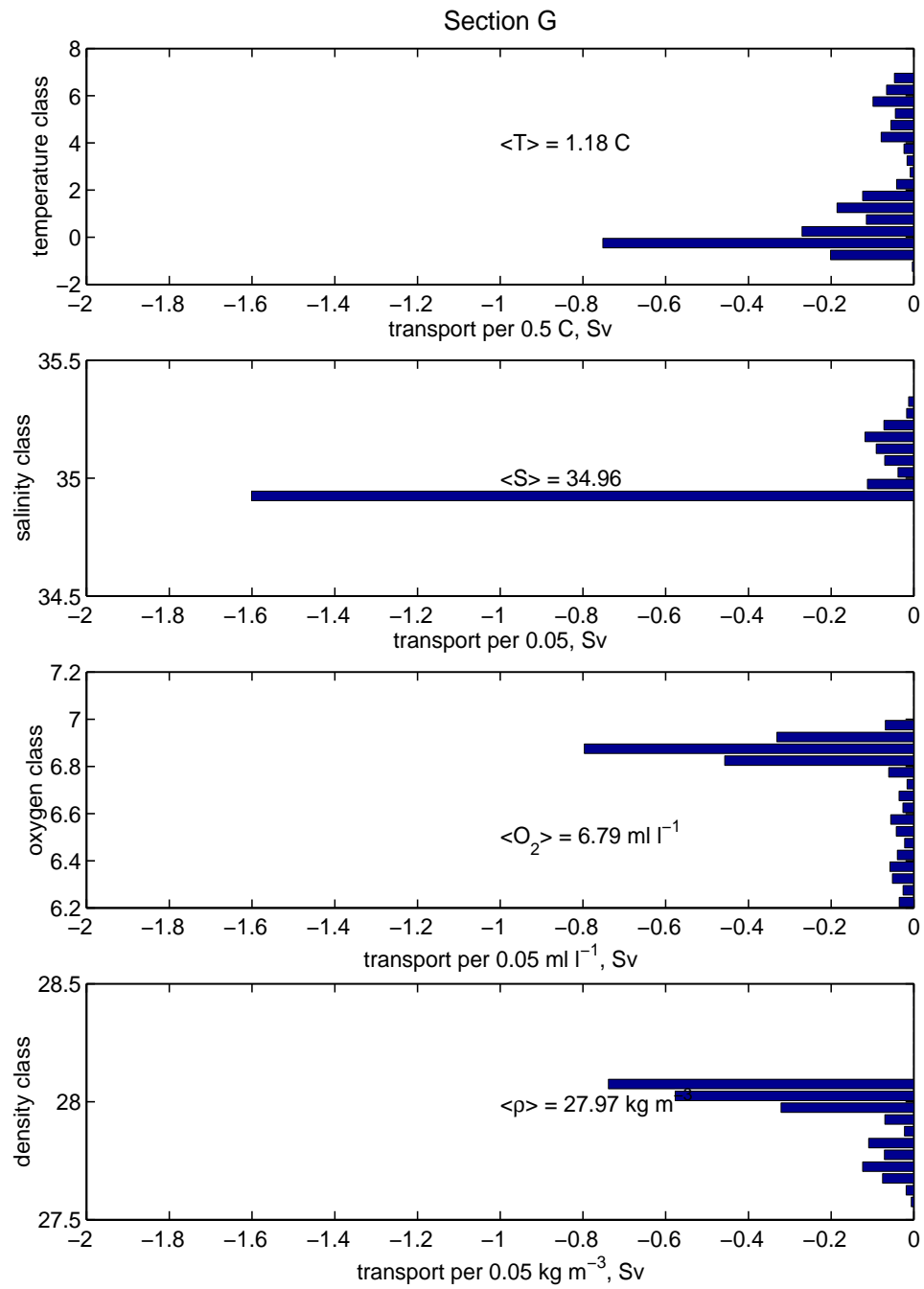


Figure 39: Transport of temperature, salinity, density and oxygen shown in variable classes across section G. Currents were measured by XCP and hydrographic variables by CTD.

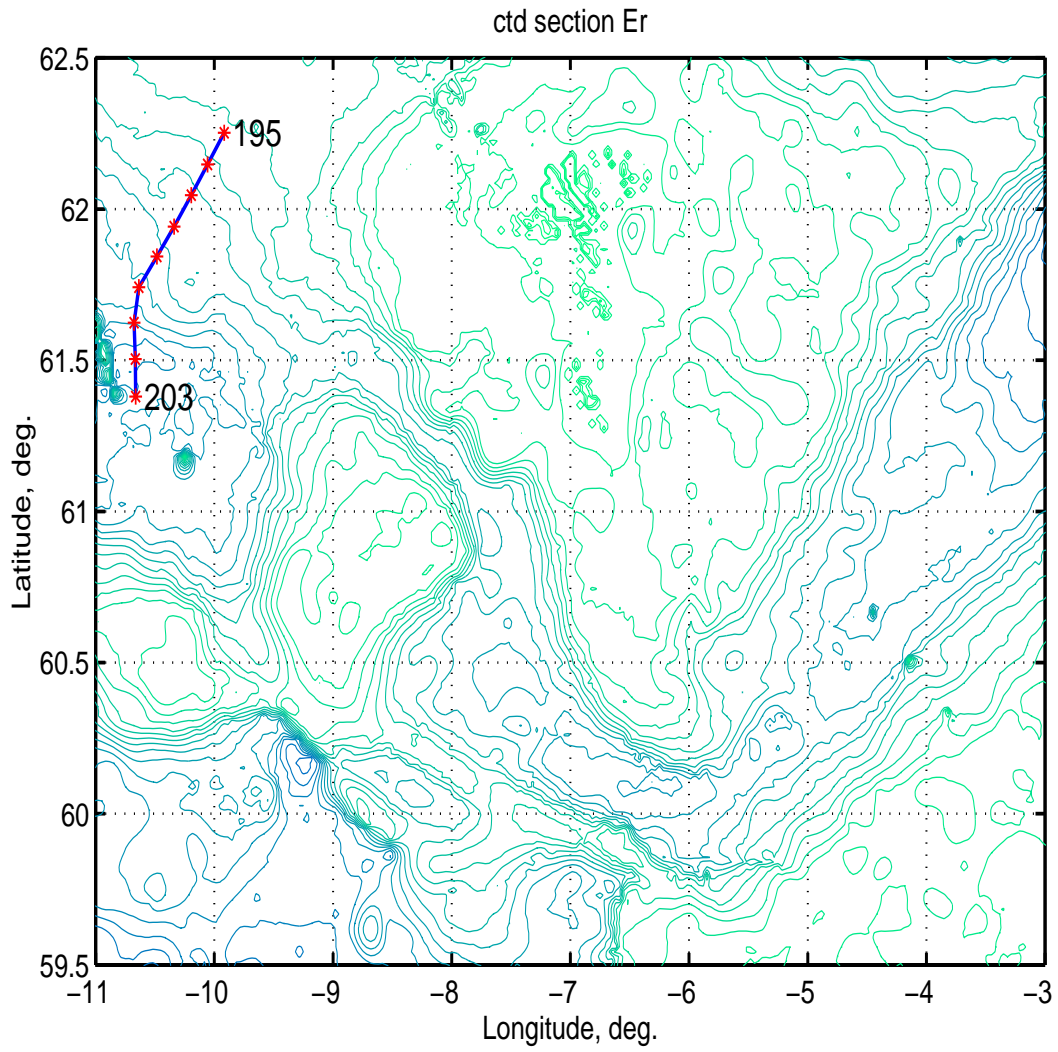


Figure 40: CTD stations along section Er, the westernmost section.

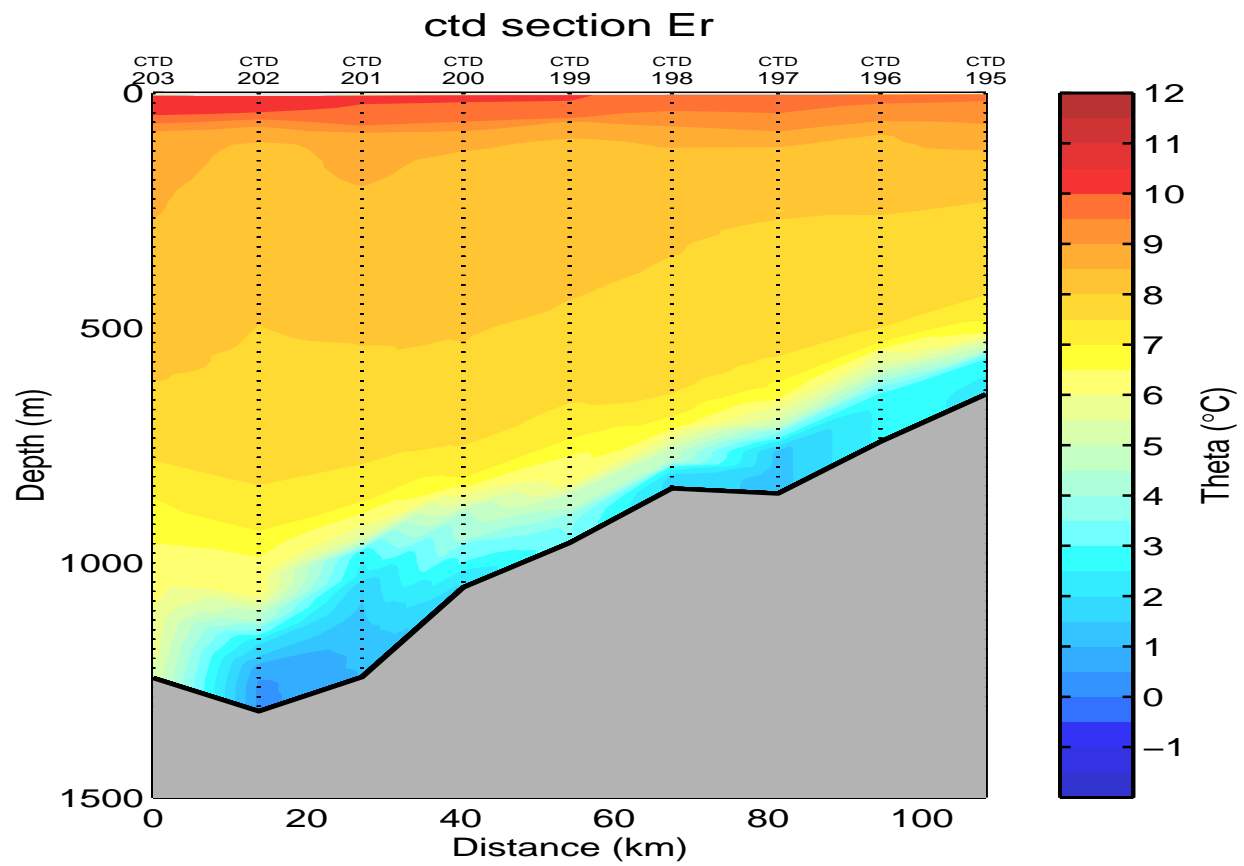


Figure 41: A section of potential temperature from section Er. (see Figure 40 for details of station locations).

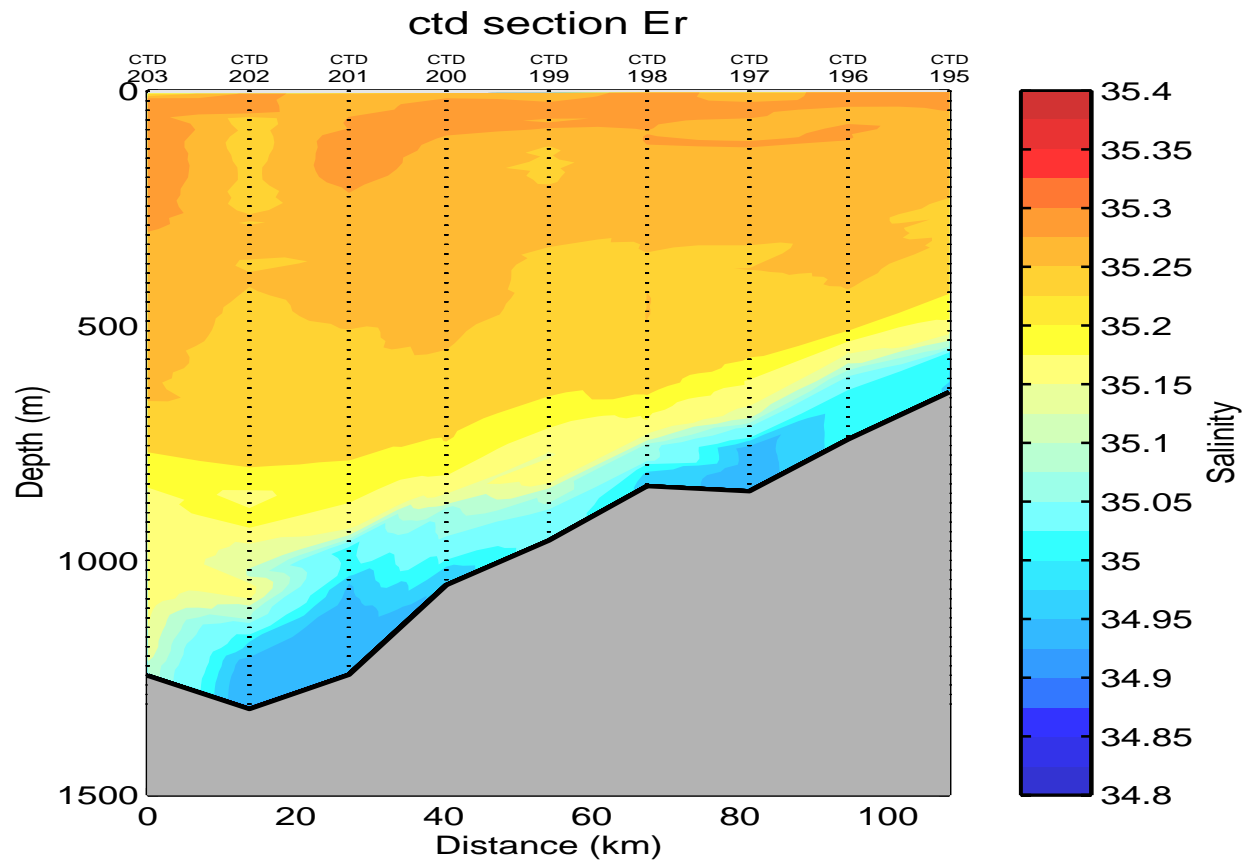


Figure 42: A section of salinity from section Er. (see Figure 40 for details of station locations).

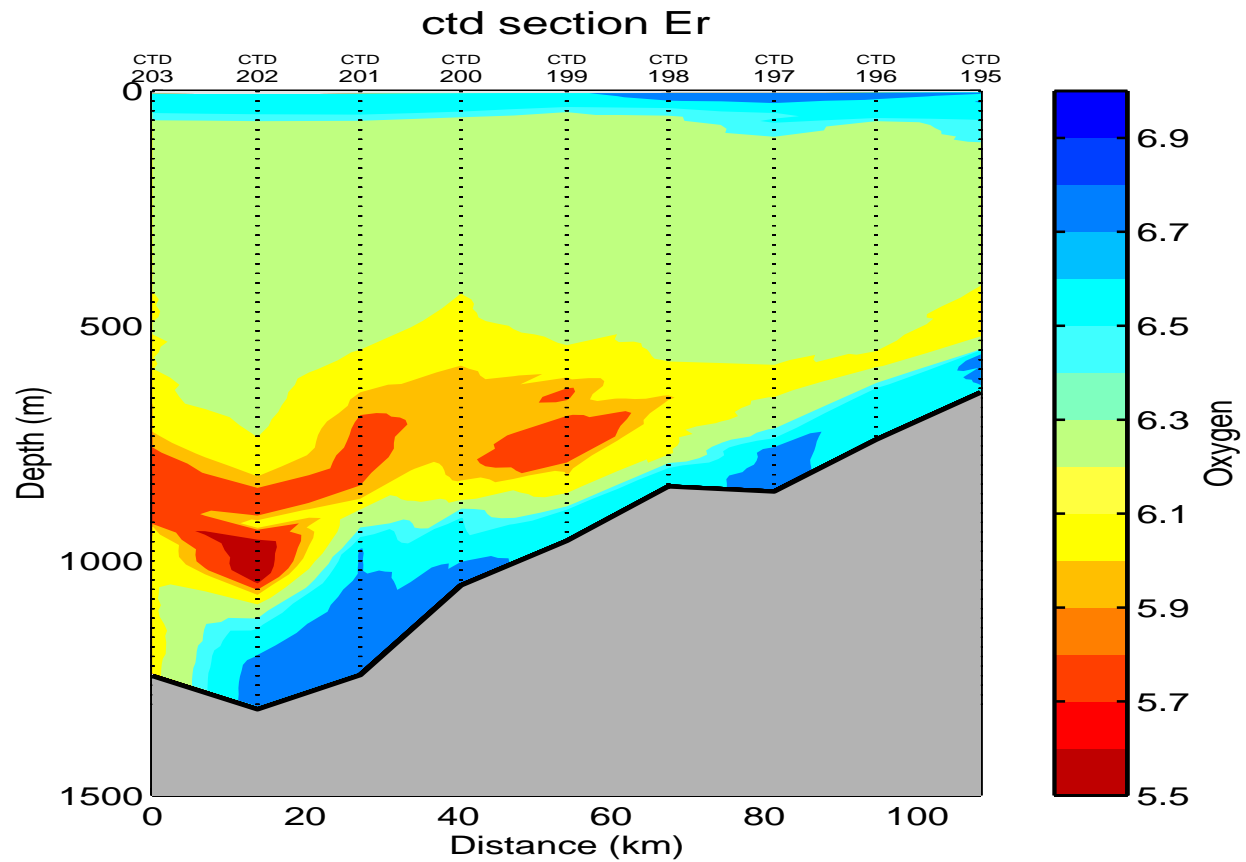


Figure 43: A section of dissolved oxygen from section Er. (see Figure 40 for details of station locations).

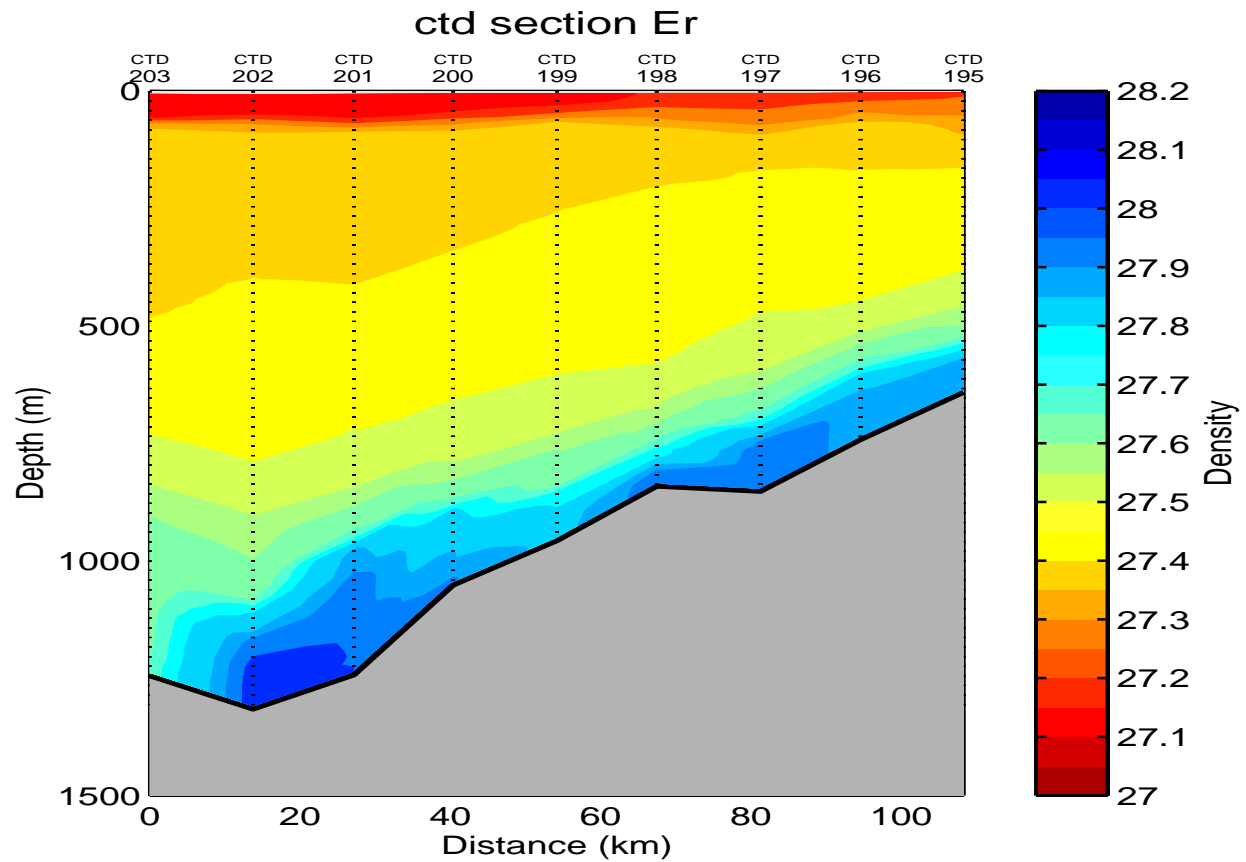


Figure 44: A section of potential density from section Er. (see Figure 40 for details of station locations).

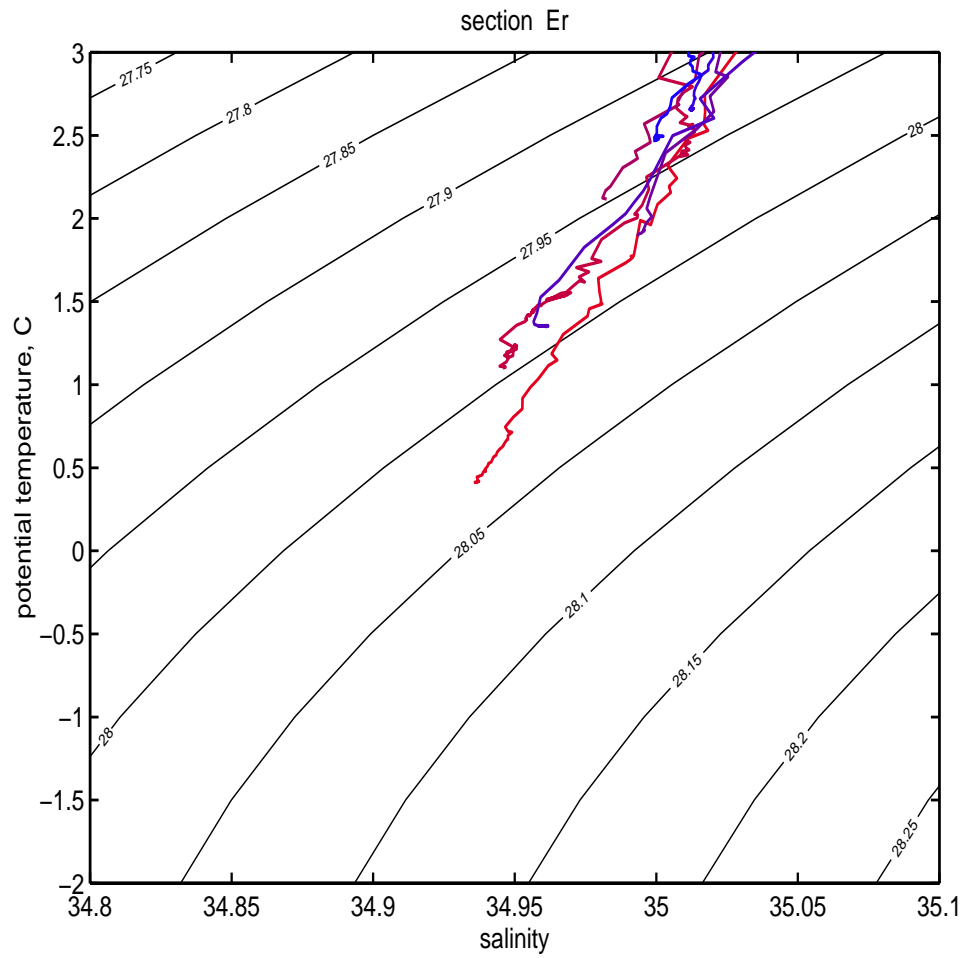


Figure 45: T-S diagram from section Er. The colors indicate west(red) to east(blue).

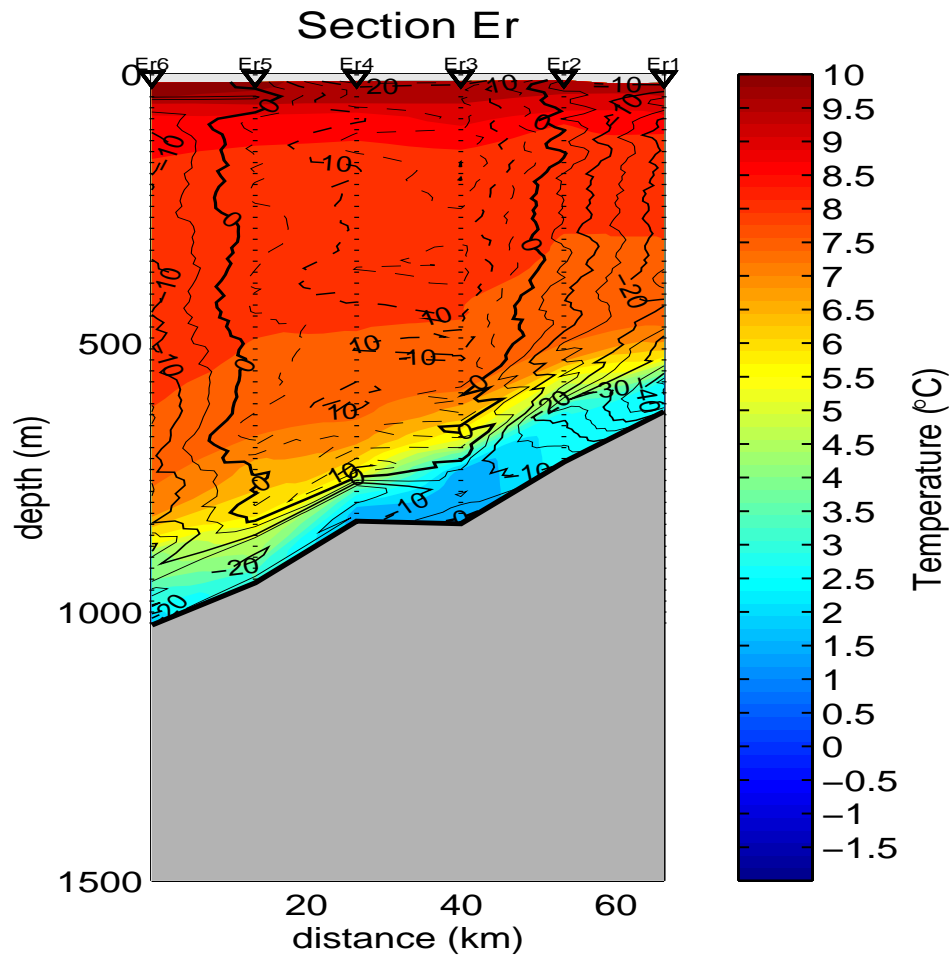


Figure 46: XCP-measured temperature (color coded) and current component normal to the section (contoured, units are  $\text{cm s}^{-1}$ ) on section Er.

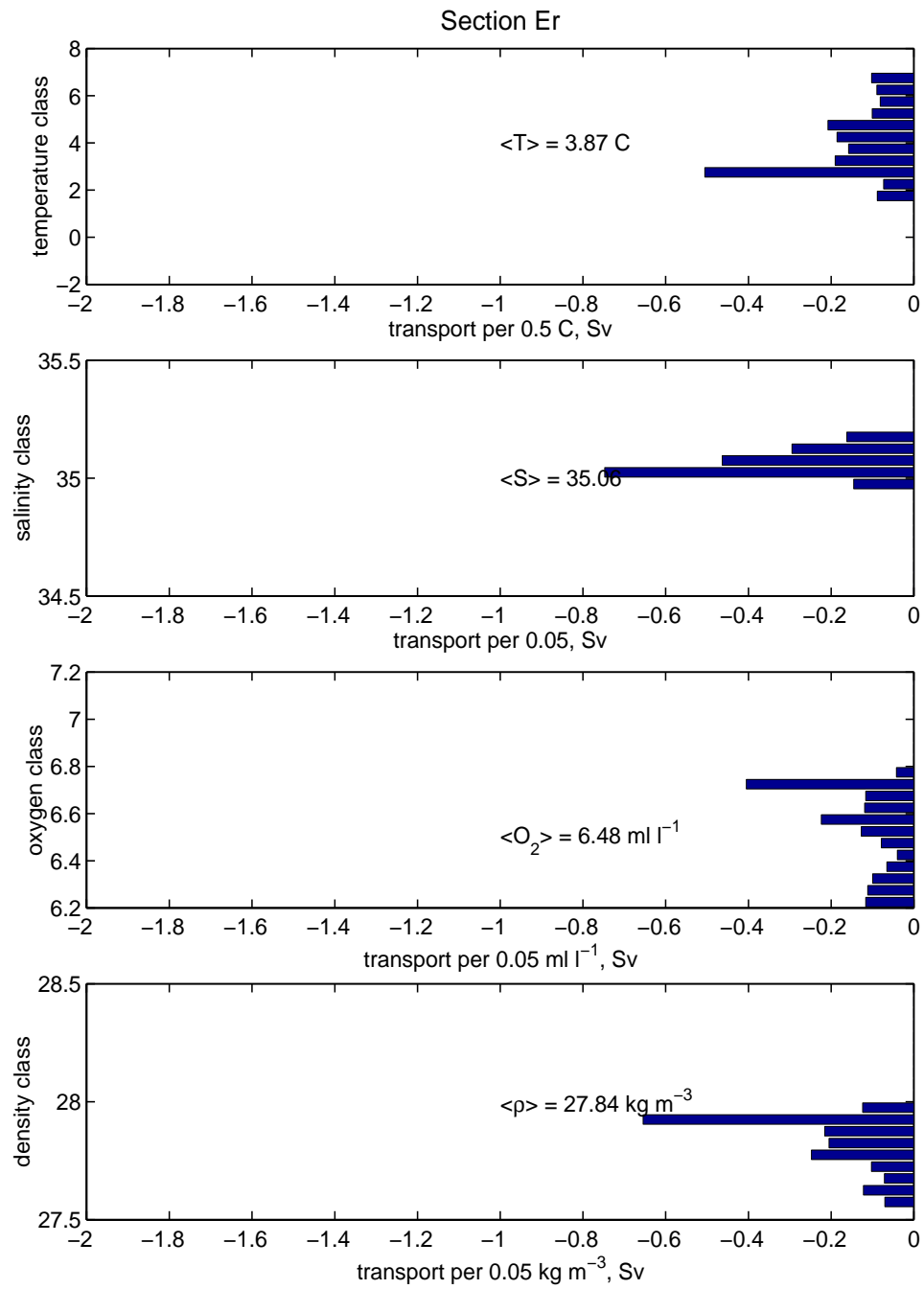


Figure 47: Transport of temperature, salinity, density and oxygen shown in variable classes across section er. Currents were measured by XCP and hydrographic variables by CTD.

## 8 A Longitudinal Section

The sections we occupied were generally transverse to the overflow. In order to assess the longitudinal structure of the overflow, we have made up a synthetic, longitudinal section, called K, by selecting stations that were in the core (maximum density and maximum thickness) as seen in the transverse sections.

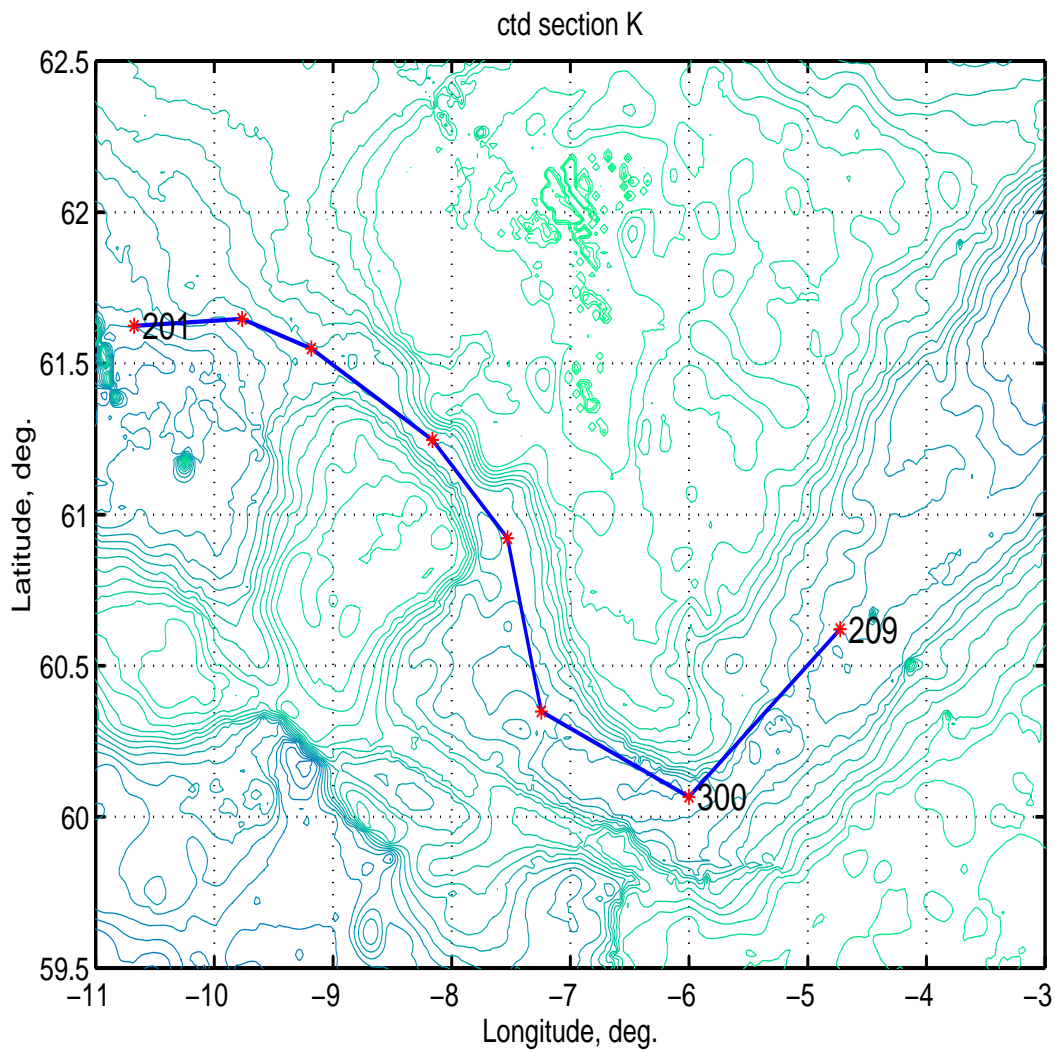


Figure 48: CTD stations along the path of the Faroe Bank Channel overflow. Station 300 is a way point only (no CTD data at that point.)

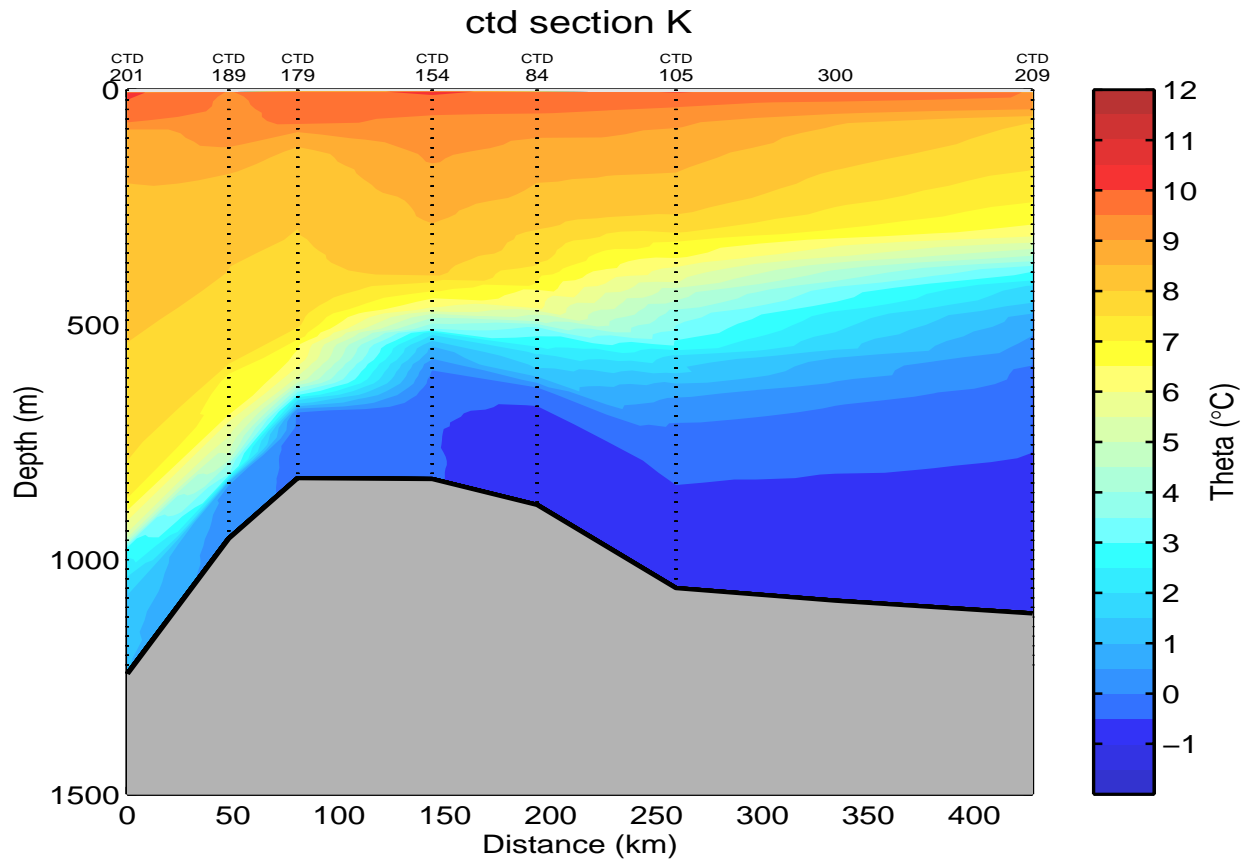


Figure 49: A section of potential temperature made up from CTD stations taken along the path of the Faroe Bank Channel overflow (see Figure 48 for details of station locations). The Norwegian-Greenland Sea is to the right, and the northern North Atlantic is to the left.

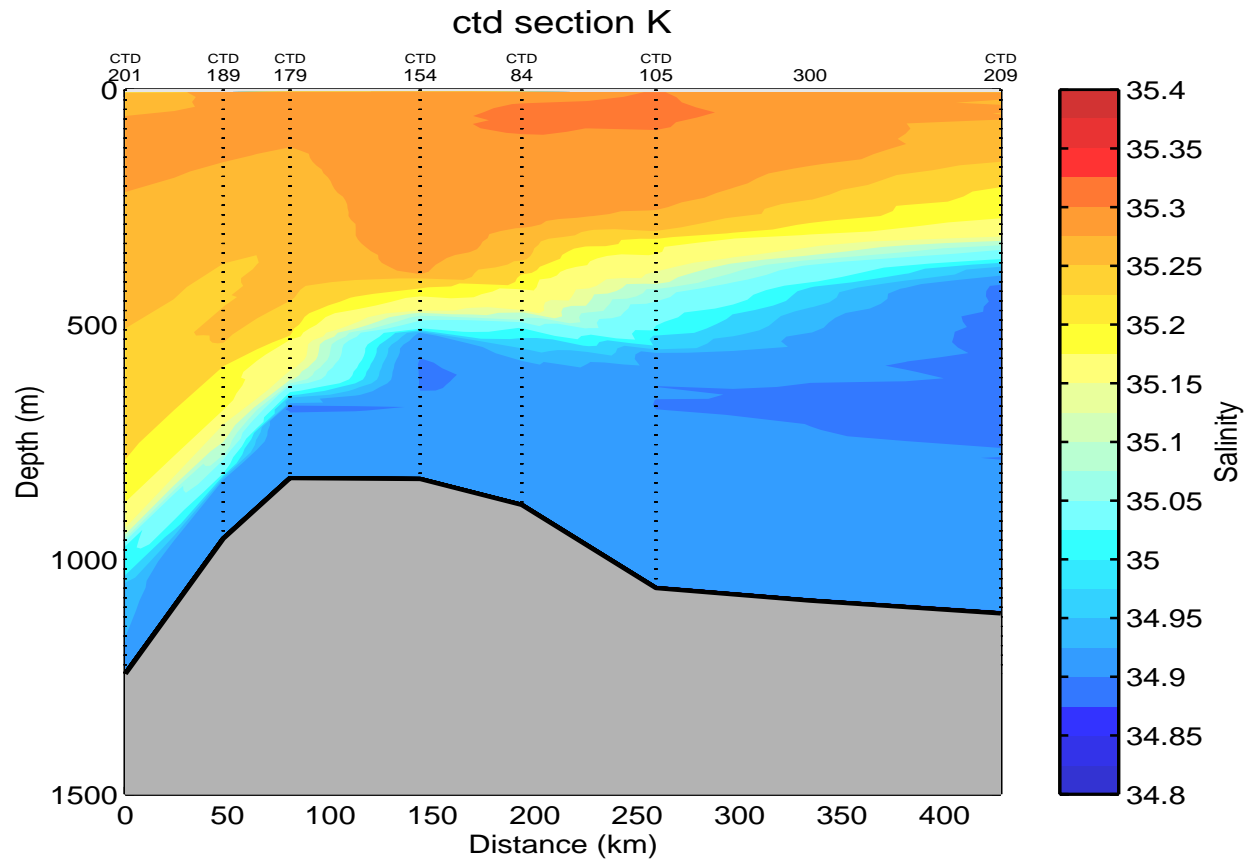


Figure 50: A section of salinity made up from CTD stations taken along the path of the Faroe Bank Channel overflow (see Figure 48 for details of station locations). The Norwegian-Greenland Sea is to the right, and the northern North Atlantic is to the left.

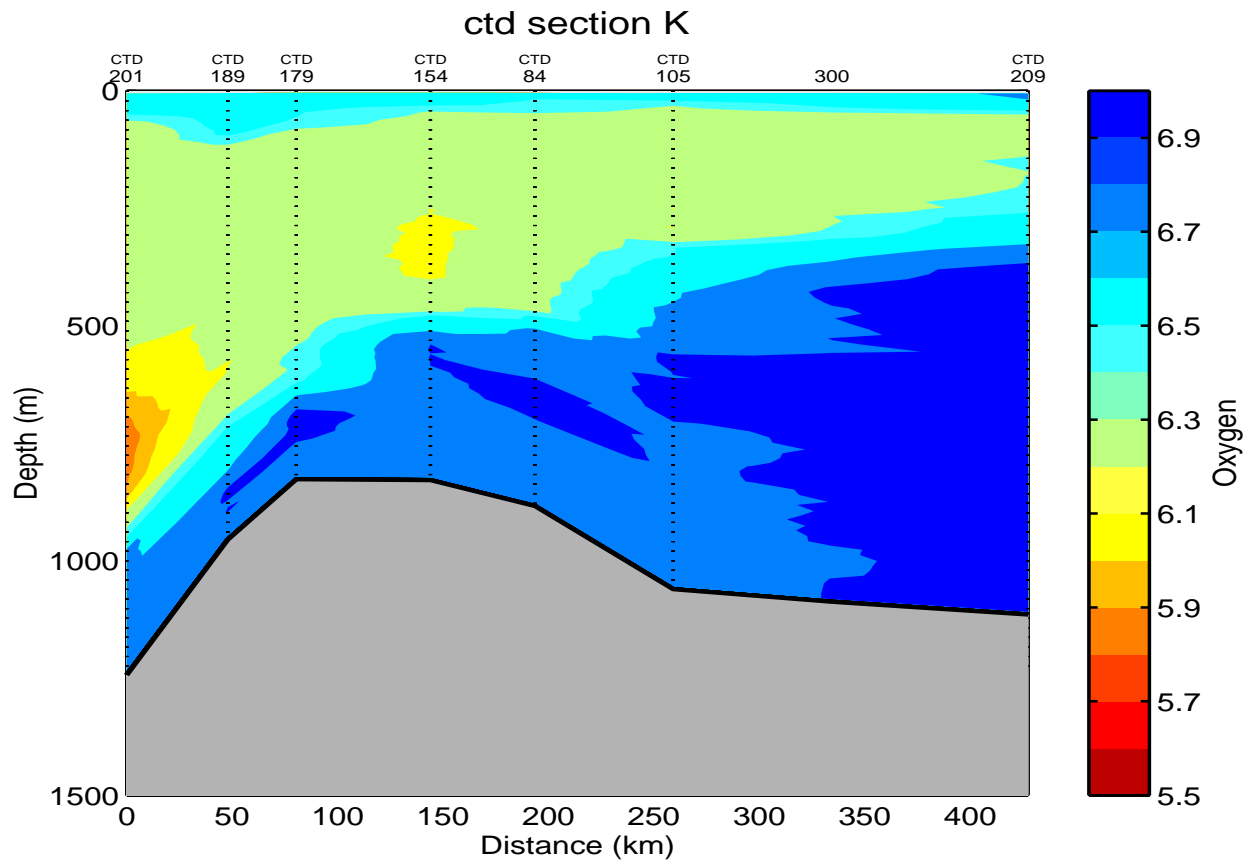


Figure 51: A section of dissolved oxygen made up from CTD stations taken along the path of the Faroe Bank Channel overflow (see Figure 48 for details of station locations). The Norwegian-Greenland Sea is to the right, and the northern North Atlantic is to the left.

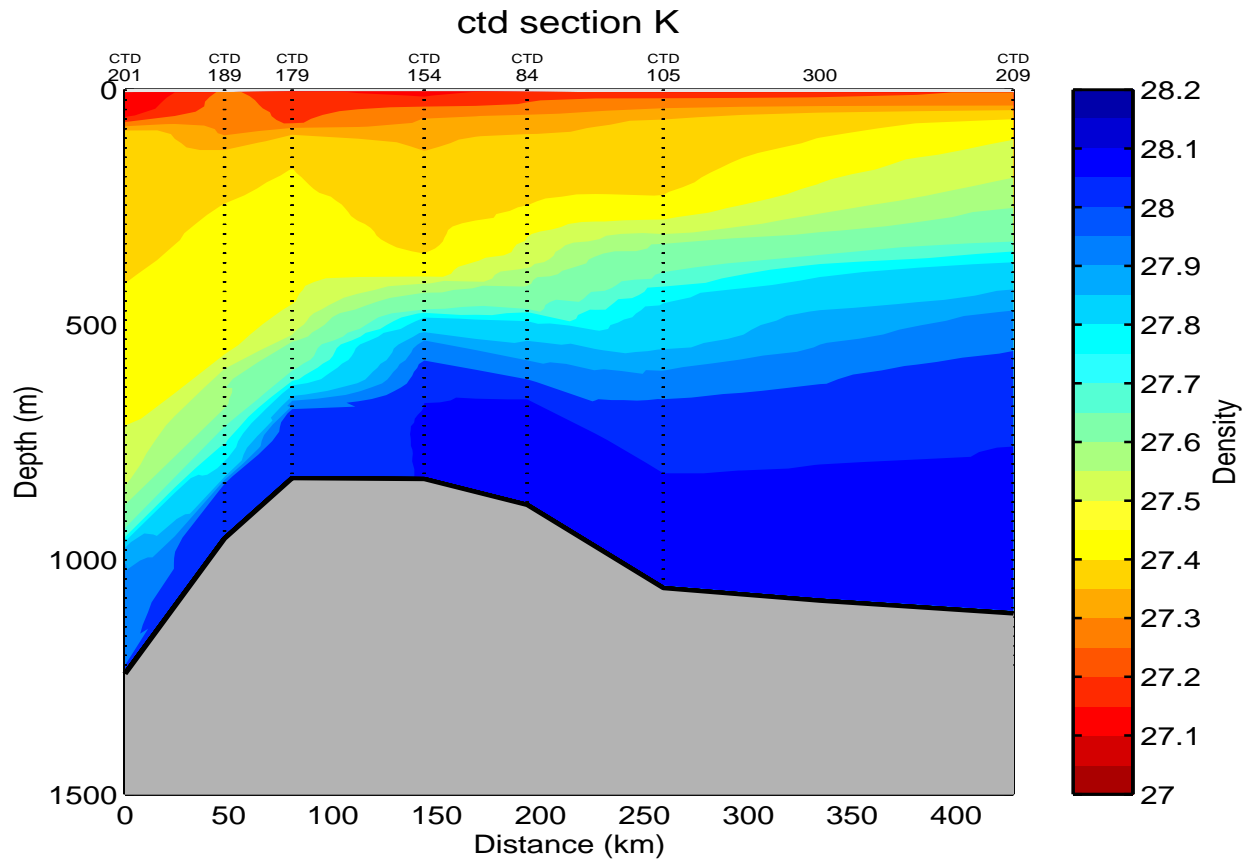


Figure 52: A section of potential density made up from CTD stations taken along the path of the Faroe Bank Channel overflow (see Figure 48 for details of station locations). The Norwegian-Greenland Sea is to the right, and the northern North Atlantic is to the left.

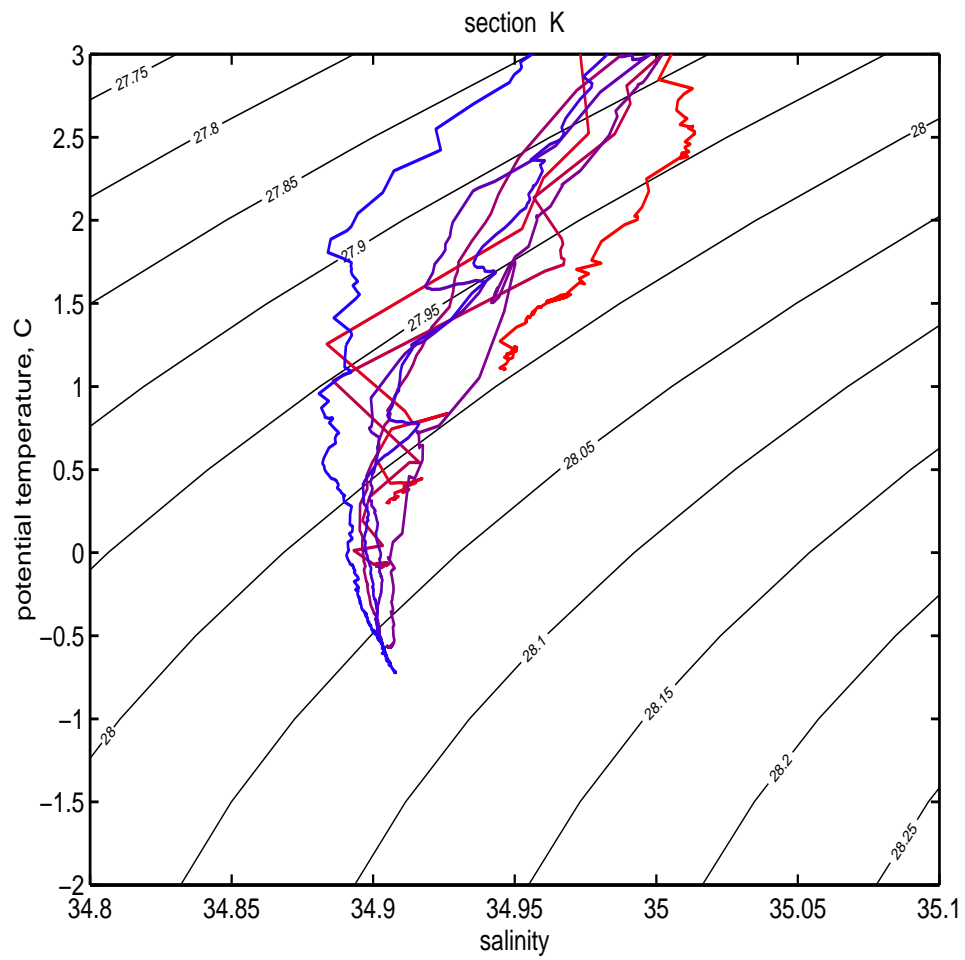


Figure 53: T-S diagram from section K. The colors indicate west(red) to east(blue).

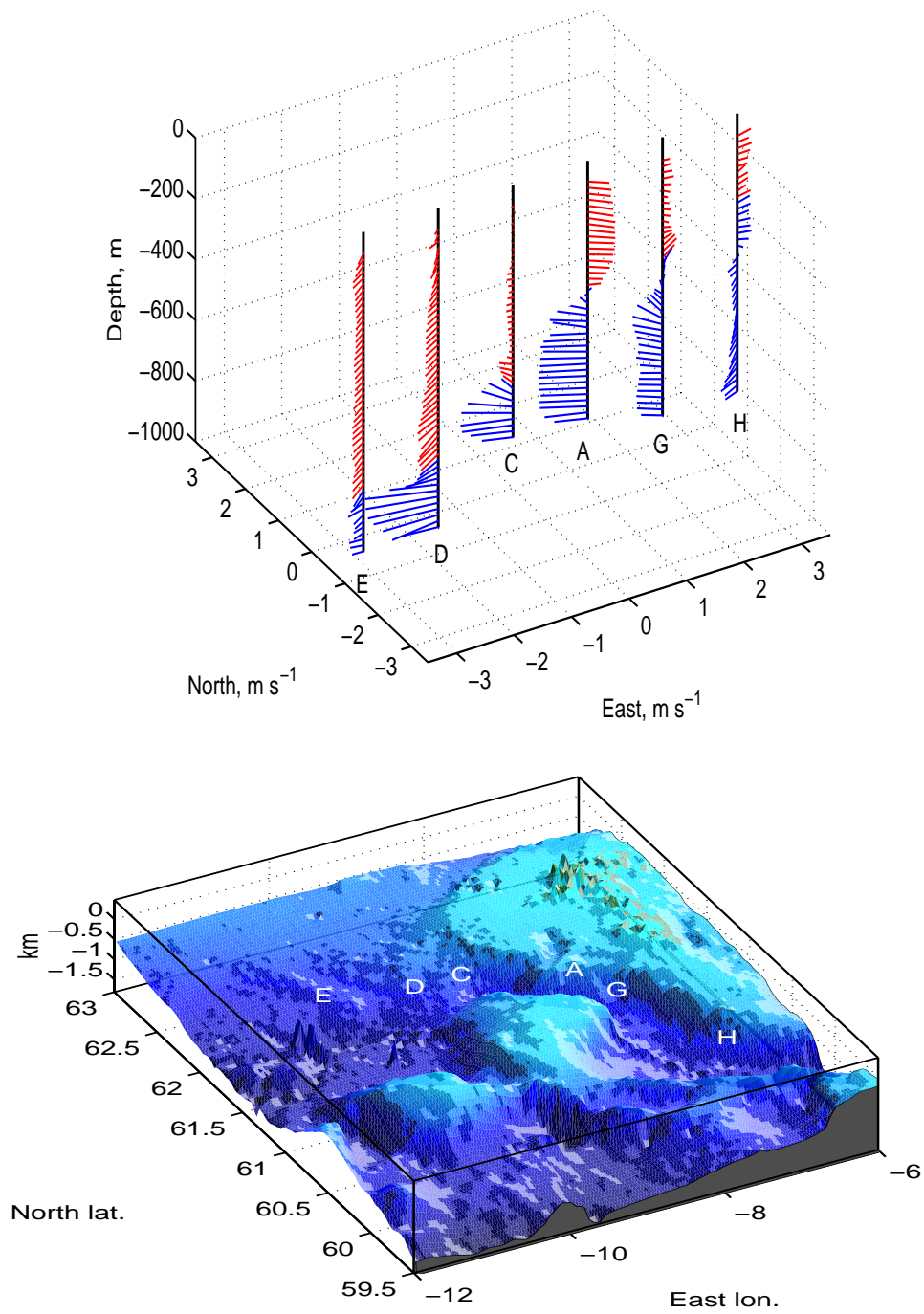


Figure 54: A 3-d perspective view of XCP currents along section K.

## 9 Velocity-weighted Property Transports.

The velocity-weighted transport of temperature, salinity, oxygen and density are shown below. These are the integral transports for the available CTD/XCP sections and show how these integral properties vary along the overflow. The date (in June, 2000) of the corresponding section is shown beside the data point.

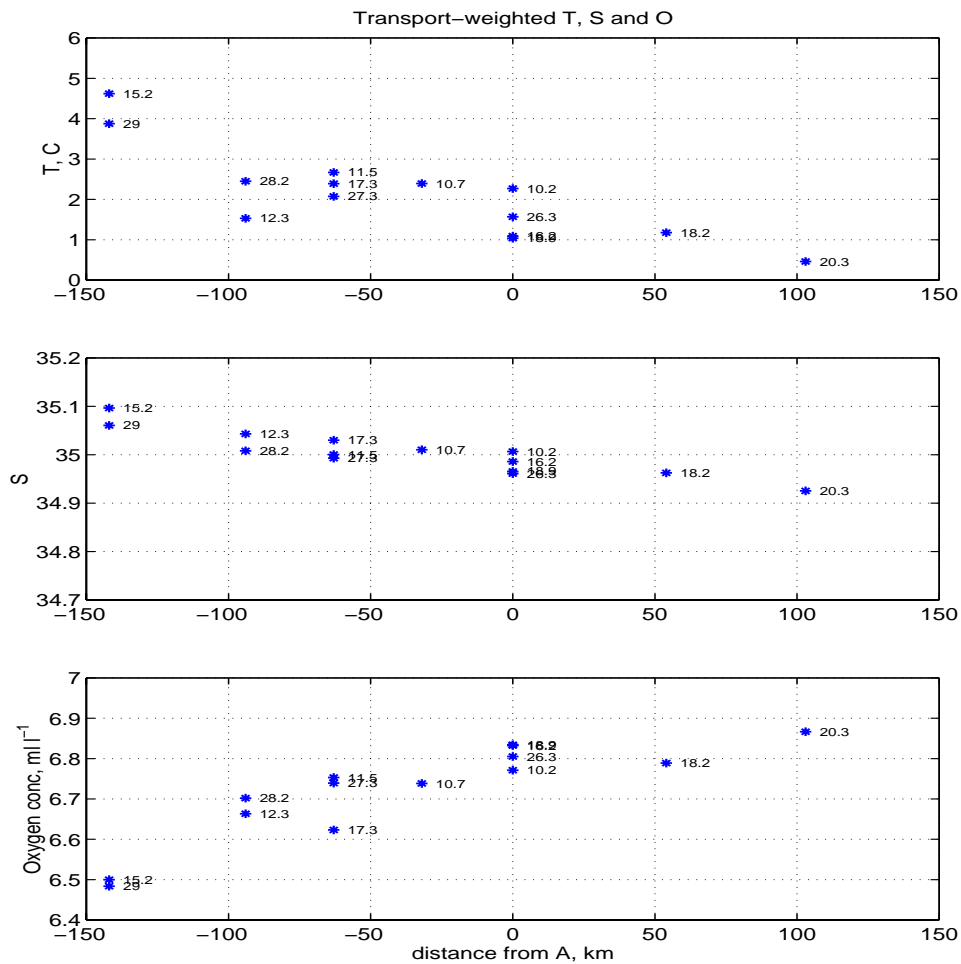


Figure 55: Velocity-weighted transport of temperature, salinity and oxygen. Each estimate corresponds to a section; the small number to the right of the data point is the date in June. These data are preliminary (even more than the rest!). Section H (easternmost) is very poorly sampled, and section E (westernmost) is incompletely sampled.

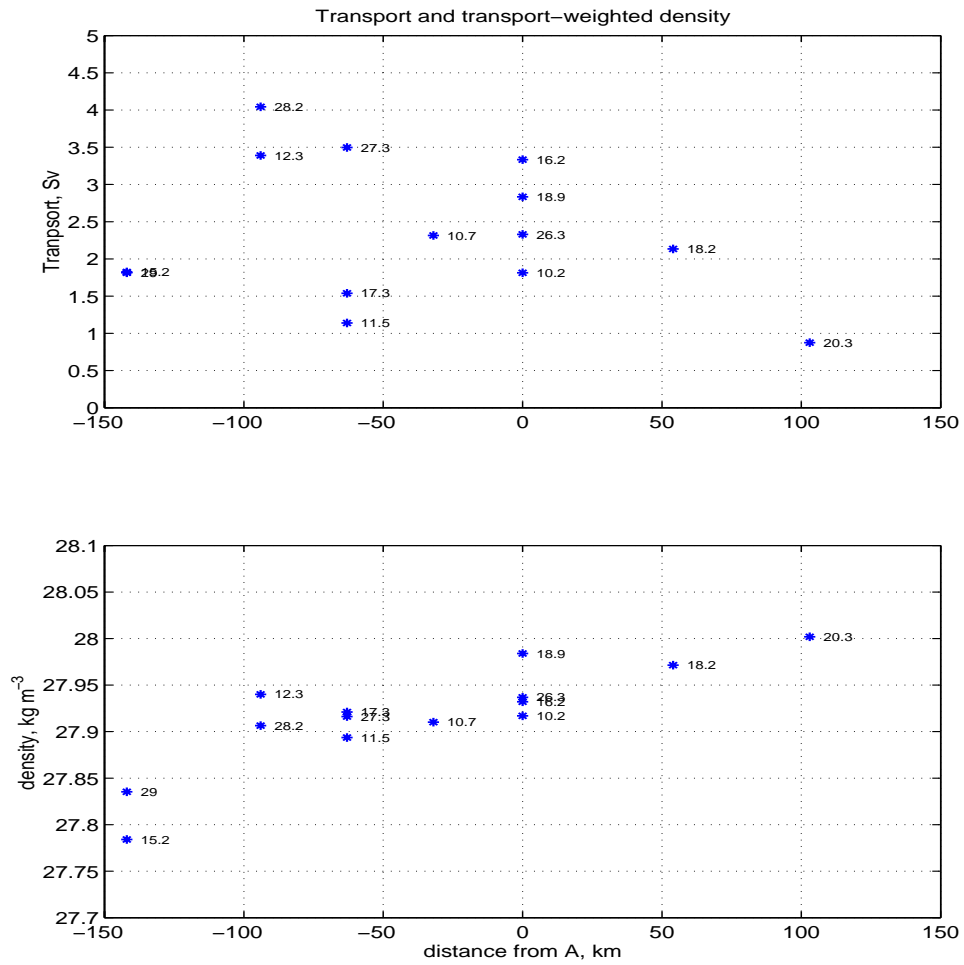


Figure 56: Transport (above) and velocity-weighted density transport (lower). Each estimate corresponds to a section; the small number to the right of the data point is the date in June. These data are preliminary (even more than the rest!). Section H (easternmost) is very poorly sampled, and section E (westernmost) is not completely sampled.

## 10 Bottom Stress Estimates

Bottom stress has been estimated from 2 db-sampled XCP data using a straightforward log-layer formulation. The data used were the deepest 10 m of the profile (assuming that the profile terminated at the sea floor) and assuming that the temperature difference over this interval was less than 0.03 C. This latter condition was intended to minimize the effects of stratification which in a few profiles was fairly large. Other values for this temperature cutoff, 0.02 and 0.01 C gave very similar results.

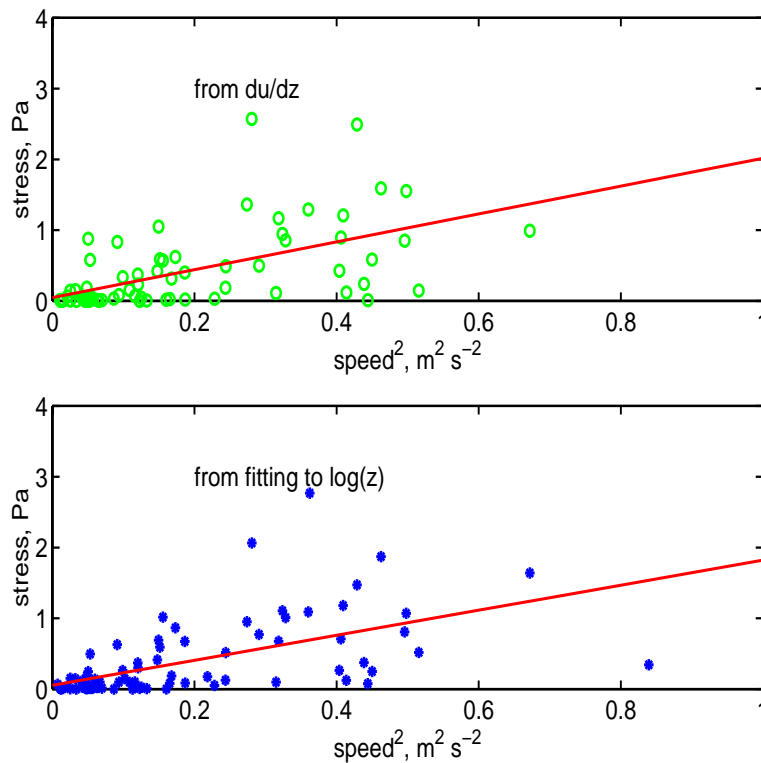


Figure 57: Bottom stress estimates from a log layer analysis of XCP data. (upper) By estimating and averaging  $du/d(\log(z))$ , and (lower) by fitting the current to a  $\log(z)$  profile. Data were from the depth range 1 to 11 m above the bottom. Profiles were excluded if the temperature difference over this depth range exceeded 0.03 C (about 20 percent of the data set). The red line is a linear least squares fit of  $\text{stress}(\text{speed}^2)$ , and the intercept at  $\text{speed}^2 = 1$  provides an estimate of the 10 m drag coefficient times density, i.e.,  $Cd_{10} \approx 2.0 \times 10^{-3}$ .

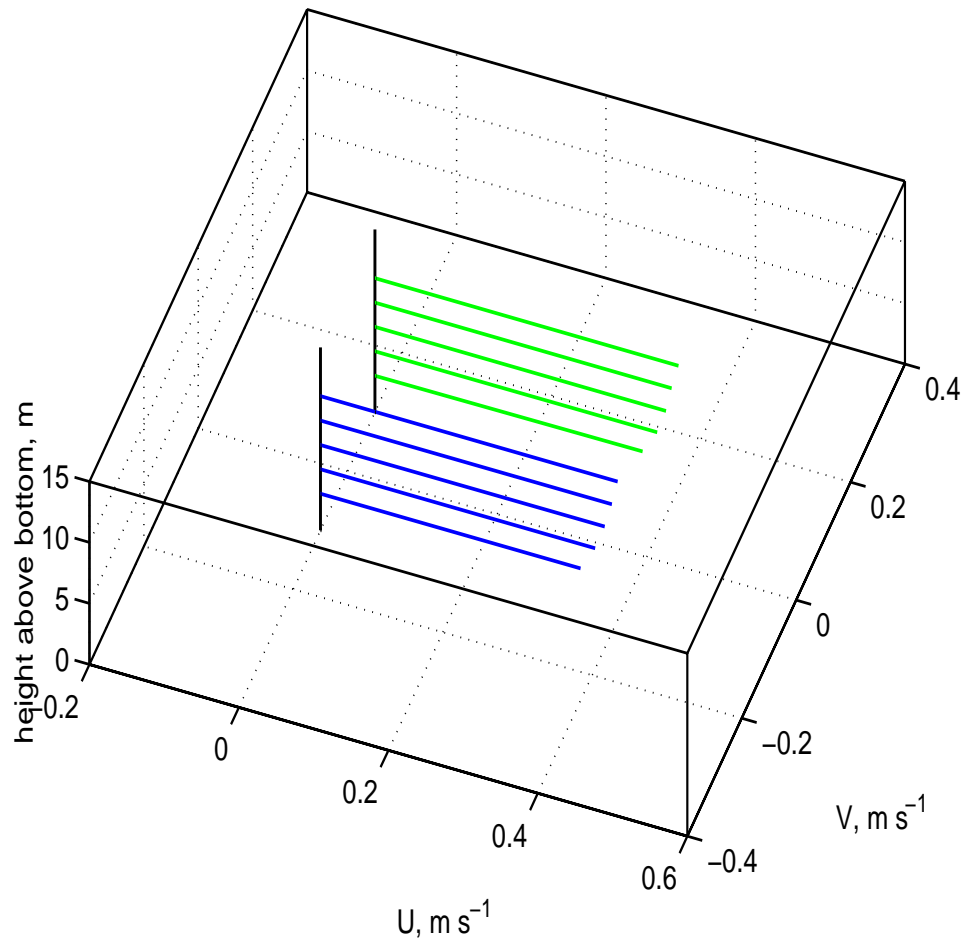


Figure 58: The ensemble average of the rotated current vectors (blue vectors) and corresponding log layer profile of current having the same average bottom stress and the  $Cd_{10}$  from Figure 57.

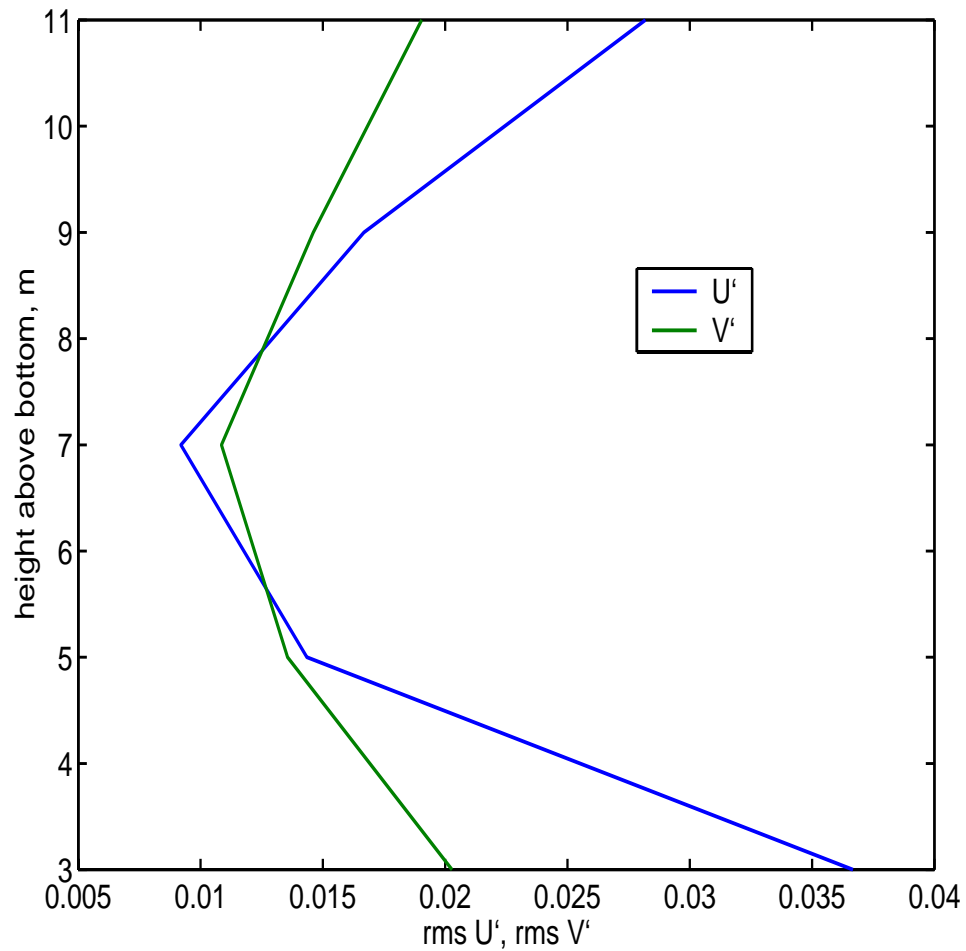


Figure 59: The ensemble average rms of the deviation of the current from a log fit to each profile. The blue line is the deviation in the along mean current direction, while the green line is the deviation in the direction normal to the mean current. Note that the rms deviation is about 5 to 10 percent of the mean current (compare this to Figure 58 where the ensemble mean current is about  $0.35 \text{ m s}^{-1}$ ). This is a reasonable variance for a wall-bounded boundary layer.